EXPERIMENTAL STUDIES OF VIBRATIONAL AND DISSOCIATIVE NONEQUILIBRIUM IN EXPANDED GAS FLOWS*

38p

by

I. R. Hurle, A. L. Russo, and J. Gordon Hall

Cornell Aeronautical Laboratory, Inc.
Buffalo 21, New York

Paper to be presented at the AIAA Conference on Physics of Entry into Planetary Atmospheres, to be held at Boston, August 26-28, 1963.

*This work is supported by AFOSR, Contract No. AF 49(638)-792; by NASA, Contract No. NASr-109; and by AFOAR, ARL, Contract No. AF 33(657)-8860.

EXPERIMENTAL STUDIES OF VIBRATIONAL AND DISSOCIATIVE NONEQUILIBRIUM IN EXPANDED GAS FLOWS*

I. R. Hurle, A. L. Russo, and J. Gordon Hall
Cornell Aeronautical Laboratory, Inc., Buffalo, New York

ABSTRACT 14968

Studies have been made of vibration and dissociation nonequilibrium effects produced in supersonic-nozzle expansions of diatomic gases from known equilibrium conditions attained behind reflected shock waves. The experiments were done in an axisymmetric, 15° conical nozzle attached to the end of a conventional shock tube. For the study of vibrational nonequilibrium without dissociation, nitrogen was shocked to reservoir temperatures and pressures in the ranges 2800 to 4600°K and 24 to 82 atm. The extent of vibrational excitation was determined by measurement of local vibrational temperatures using the spectrum-line reversal method. For the study of dissociation nonequilibrium without significant vibration, hydrogen-argon mixtures were shocked to a reservoir temperature of 6000°K and pressures from 28 to 112 atm. At these conditions the hydrogen ($\sim$ 8% mole fraction) was almost completely dissociated. Nozzle-wall pressure distributions were measured to observe effects due to nonequilibrium H_2 dissociation.

The studies of N_2 vibration by the spectrum-line reversal method showed the vibrational temperatures in the nozzle flows to be much closer to equilibrium than the available relaxation theory predicts. Observations at two nozzle area ratios showed that vibration was not completely frozen. The rates of vibrational de-excitation inferred from these measurements on the basis of current theory are about fifteen times greater than those inferred from previous measurements made behind normal shock waves. Possible reasons for this difference are discussed in terms of the basic differences between shock-wave and nozzle-expansion flows, and the applicability of Landau-Teller assumptions to the latter conditions.

The wall pressure measurements made in the studies of dissociated H_2 + Ar expansions showed a consistent reduction from equilibrium values. This reduction in static pressure is attributed to the occurrence of a lag in hydrogen atom recombination during the flow expansion. The relative insensitivity of the static pressure to the flow chemistry, together with the scatter of the experimental data, permit a determination of recombination-rate constants only to somewhat better than a factor of 2.5. Within this order of variation, at least, the recombination rate constants indicated by matching finite-rate calculations with the measured pressures are consistent with those inferred from previous shock-wave dissociation studies.

*This work is supported by AFOSR, Contract No. AF 49(638)-792; by NASA, Contract No. NASr-109; and by AFOAR, ARL, Contract No. AF 33(657)-8860.

NOMENCLATURE

A = nozzle cross-section area
A^* = nozzle cross-section area at throat
k_r = recombination rate constant
M = local Mach number
p = local pressure
Re_x = local stream Reynolds number, $\frac{\rho u x}{\mu}$
T = local translational temperature
T_v = local vibrational temperature
T_w = local wall temperature
T_0 = background or source temperature
u = local stream velocity
x = axial distance measured from nozzle throat
γ = specific heat ratio
δ^* = displacement thickness of nozzle wall boundary layer
λ = characteristic relaxation length for vibration, $= u\tau$
ρ = local stream density
τ = characteristic relaxation time for vibration
τ_s = characteristic relaxation time for vibration from Fig. 4

Subscript

0 = reservoir value, attained behind reflected shock wave

1. INTRODUCTION

The present paper describes experimental studies of vibration and dissociation nonequilibrium effects produced in supersonic nozzle expansions of diatomic gases.* The motivation for the work stems from the importance of these relaxation phenomena in various expansion-flow problems of current technical interest. While the nonequilibrium behavior of expansion flows in nozzles, for example, can be calculated by machine methods if the phenomenological description of the rate processes is known[2-5], approximations or extrapolations in the kinetic description are inevitably necessary. These extrapolations can only be truly assessed or justified by direct experiment. As an example, rate data determined from normal shock-wave (shock-tube) experiments are usually employed in calculating the nonequilibrium behavior of nozzle flows. However, the thermogasdynamic environment and the net direction of the rate processes involved, are generally very different in a nozzle flow than in a normal shock-wave flow. In the opinion of the present authors, the limitations of current knowledge of nonequilibrium molecular processes necessitate caution in making or accepting such extrapolations. There is a need for direct experimental confirmations where feasible. This view is not unique herein as

*Preliminary results from this study were previously reported in Ref. 1.

is evidenced by the increased research effort of late on nonequilibrium effects in nozzle-flow experiments[6-8].

The present experiments entail shock-wave heating of various test gases to known equilibrium states in the region behind reflected shock waves. This region serves as a reservoir for the steady-flow expansion of these gases, of millisecond duration, in a convergent-divergent supersonic nozzle coupled to the end of the shock tube. The diagnostic techniques employed in these studies include the measurement of vibrational temperatures by spectrum-line reversal and the measurement of nozzle-wall pressure and heat transfer distributions at several stations along the nozzle. Following a detailed description of the shock tube-nozzle apparatus and the measurement techniques in Sec. 2, two separate experiments will be described in Secs. 3 and 4. These two experiments involve molecular vibrational de-excitation or atom recombination, respectively, as the dominant nonequilibrium process of interest. As noted above, these two processes are of fundamental importance in various expansion flows which may entail great chemical complexity. The present experiments provide examples of simple expansion flows wherein a single nonequilibrium process dominates and observed effects can be interpreted with some confidence.

In the vibrational de-excitation studies of Sec. 3, pure nitrogen was expanded from equilibrium reservoir temperatures and pressures in the range 2800° to 4600°K and 24 to 82 atm. The intent here was to observe vibrational lag effects in a simple expansion-flow system and, in particular, one uncomplicated by chemical change. At the above reservoir conditions, nitrogen dissociation is negligible but the vibrational excitation is large. Local vibrational temperatures and wall static pressures were measured at various area ratios along the nozzle. The measurements show that vibrational excitation departs rapidly from local equilibrium at an early stage in the expansion and tends to become frozen. The local vibrational temperatures measured are considerably lower than values predicted from the simple vibrational relaxation theory (i.e., they are closer to equilibrium), although they typically exceed corresponding values appropriate to full equilibrium by 50% or more.

The present studies with nitrogen thus give only qualitative confirmation to previous theoretical analyses which predict vibration freezing in such an expanding flow system (see, for example, Ref. 5). These analyses use the vibrational relaxation theory employed to describe vibrational excitation behind normal shock waves[9]. Quantitatively, as noted above, the local vibrational temperatures measured in the present experiments are substantially below those predicted by this theory. Accordingly, these results imply that the efficiency of the vibrational de-excitation process involved in the present nozzle expansions of nitrogen is significantly higher than that inferred from measurements made behind normal shock waves[9]. Interpreted in terms of a vibrational de-excitation rate on the basis of current relaxation theory, the present results imply a rate about fifteen times faster than that inferred from appropriate shock-wave data. The question of the applicability of the latter data under the present expansion-flow conditions is discussed in Sec. 3.3.

In the chemical recombination studies described in Sec. 4, a mixture of hydrogen ($\sim$ 8% undissociated mole fraction) and argon was expanded from an equilibrium reservoir temperature of 6000°K and reservoir pressures from 28 to 112 atm. At these reservoir conditions the hydrogen was almost completely dissociated. Because of this, and the very high natural frequency of vibration of the hydrogen molecule, the energy in vibrational excitation at the reservoir conditions was very small relative to that in dissociation. Consequently, in these expansions a lag in (hydrogen) atom recombination was expected to be the dominant nonequilibrium process. The effect of this process on the flow static pressure was expected to be large (in contrast to the N_2 vibration studies). In these experiments, therefore, wall static pressure distributions only were measured. The measured pressure distributions were compared with corresponding theoretical distributions calculated for equilibrium, frozen, and finite reaction-rate flow.

When corrected for nozzle-wall boundary layer effects, the comparison shows the experimental pressures to be generally below the limit for equilibrium hydrogen dissociation but above the limit for frozen dissociation. The reduction of the pressures below corresponding equilibrium values is attributed to the occurrence of a lag in hydrogen atom recombination during flow expansion. The relative insensitivity of static pressure to the flow chemistry, together with the scatter of the experimental data, permit a determination of recombination rate constants only to somewhat better than a factor of 2.5. Within this order of variation, at least, the recombination rate constants inferred by matching finite-rate calculations with measured pressures are consistent with those inferred from previous shock-wave dissociation studies. However, any incompatibility with shock-wave rate data within this factor, analogous to what is observed for nitrogen vibration, would be masked by the data scatter.

2. EXPERIMENTAL METHOD

2.1 Shock Tube and Nozzle Apparatus

The shock tube used is of conventional design and consists of a high-pressure driver-gas tube and low-pressure driven or test-gas tube separated by a double-diaphragm section. The driver is 12 ft. long, 3-1/2 in. I.D., and is capable of operation at driver-gas pressures up to 30,000 psi. Helium and hydrogen were both used as driver gases in the present work. The driven tube is 20 ft. long with a square internal cross-section 2-1/2 x 2-1/2 in., and has a maximum working pressure of 5000 psi. The double-diaphragm section allows controlled bursts of the main driver diaphragm at desired driver-gas pressures. This technique has resulted in a high degree of reliability and reproducibility in obtaining the desired reservoir conditions at the nozzle entrance.

The downstream half of the driven tube is instrumented with thin-film resistance thermometers which are used as time-of-arrival gages for the incident shock wave. In addition, the last station in the driven tube, about 3-5/8 in. from the nozzle entrance, is instrumented for pressure

measurement and also contains small viewing windows for spectroscopic measurements. The initial test-gas pressure is monitored on a bank of four Wallace & Tiernan precision manometers with overlapping scales covering the pressure range from 0 - 800 mm Hg abs.

The axisymmetric nozzle used in the present work is coupled to the end of the shock tube and discharges into a large tank. Schematic views of both the nozzle and the assembled apparatus are shown in Fig. 1. The nozzle has a 3/8-inch diameter throat, upstream of which the contour rapidly becomes plane and normal to the tube axis to provide good reflection of the incident shock wave. A few inches downstream of the throat the contour becomes conical with a total included angle of 15°. The entire contour is smooth to the extent that the second derivative is continuous throughout.

The nozzle can be instrumented along the walls to permit the simultaneous measurement of static pressure and heat transfer, and small windows are fitted to allow optical measurements. At present, nozzle-wall static pressure distributions can be obtained from measurements at area ratios of $A/A^* = 4$, 8, 16, 32, 64 and 128, as indicated in Fig. 1. Spectroscopic line-reversal measurements can be simultaneously obtained at area ratios of 8 and 32.

Prior to each experiment the nozzle and discharge tank are isolated from the shock tube by means of a scribed copper diaphragm located at the nozzle entrance. The nozzle-tank combination is evacuated to less than 0.1μ Hg and has a maximum rate of pressure rise of 0.1μ Hg per minute. The driven-gas tube is initially evacuated to less than 0.2μ Hg prior to charging with test gas to the desired initial pressure. The driven tube has a measured leak rate of about 1μ Hg per minute. Following the bursting of the driver-driven gas diaphragm, the pressure rise behind the reflected shock wave at the end of the driven tube is sufficient to burst the copper diaphragm (but not fragment it). Thereupon, steady flow is established through the nozzle in a time of the order of a few hundred microseconds.

2.2 Temperature Measurement

The measurement of temperature in a nonequilibrium system, when possible, affords a powerful means of studying the behavior of associated nonequilibrium processes. Of course, such systems cannot be characterized by a single temperature. However, the various degrees of freedom, if in Boltzmann distributions, may be characterized by widely differing but meaningful temperatures. This is the case in the nonequilibrium expansion flows of undissociated N_2 considered in the present work. In these flows, the lag in vibrational de-excitation produces local vibrational temperatures which are considerably higher than the local equilibrated translational and rotational temperatures, while its effect on the normal observable thermodynamic properties is small. Hence, a measure of the vibrational temperature will provide the most sensitive and direct determination of the nature and efficiency of the processes of vibrational de-excitation under these conditions. The spectrum-line reversal method described below has been previously shown to measure vibrational temperatures in nonequilibrium systems[17], and was accordingly used to record the vibrational temperatures in the present N_2 expansions.

Spectrum-Line Reversal Method - Due to the strong dependence of radiation intensity on temperature, the most sensitive and acceptable determination of the temperature of a gas is provided by a measure of the light which it emits or absorbs. An accurate temperature measurement using absolute or relative emission intensities of spectral lines or bands requires a detailed knowledge of the density and radiative strengths of the emitting species, and is complicated by the varying effects of self-absorption. While the latter complication is avoided by measuring the intensities in absorption, the others remain. However, if a simultaneous measurement is made of both emission and absorption intensities these difficulties can be avoided entirely, and the temperature of the gas may be accurately determined. The observation may then also be restricted to a single convenient spectrum line or band, and can be made photometrically to obtain time-resolved temperatures. (The resonance lines of the metallic atoms Na and Cr are most suitable in this respect.) This is the essence of the line reversal method as adapted to the measurement of transient gas temperatures. The principles of this method have been described in detail by Gaydon and Hurle[10], and only an account of its present experimental application and the effective temperature it measures is given here.

Optical System for Line-Reversal Measurements - The optical arrangement used for reversal measurements in the present work is shown in Fig. 2(a). Light from a continuous background source S_1 is focused by the lens L_1, via beam splitter B_1 and window W_1, into the nozzle. A portion of the image S' formed on the nozzle axis is focused by the lens L_2, via beam splitter B_2 and aperture A_1, on to the aperture A_2. This precedes an interference filter F_1 which covers the exposed cathode area of the photomultiplier P_1. The filter F_1 is used to isolate a narrow wavelength region around the spectrum line concerned. The apertures A_1 and A_2 ensure that P_1 receives light from the same area, and in the same solid angle, for both the image S' and the radiating gas in the nozzle. It is vitally essential that this condition is fulfilled, otherwise the emission from the gas will be overweighted and the measured temperature will then be erroneously high.

The second photomultiplier P_2 is sighted along an identical reciprocal path $P_2 - S'$, so that the emission is observed from exactly the same volume of gas as the absorption. This optical arrangement removes any possible error due to non-isotropic properties of the observed gas sample. The source S_2 is similar to S_1, but is used only to balance the sensitivities of the two optical beams prior to an experiment. For this purpose it is set at a brightness temperature equal to that of the main source S_1, and the photomultiplier output signals adjusted to be equal. This procedure compensates for any optical and electronic inequalities between the two recording systems.

The photomultiplier signals are displayed on a double-beam Tektronix Model 502 oscilloscope,

the upper and lower beams displaying respectively the emission upwards and absorption downwards. A typical oscilloscope record obtained in the present work is shown in Fig. 5, and the evaluation of the temperature from this record is described in Sec. 3.1.

Two similar double-beam systems are used to permit the vibrational temperature to be determined simultaneously at area ratios of 8 and 32 in the nozzle. The arrangement of these beams is shown in Fig. 2(b), in which the outer beams are obtained by the use of the first-surface mirrors M_1 and M_2. Only one of these outer beams was used in the present work. The windows W_1 and W_2 are 1-inch diameter and 1/4-inch thick quartz discs, mounted tangent with the inside surface of the nozzle wall. The optical path lengths at the two stations are about 1 and 2 inches, respectively.

The background sources consist of small tungsten spheres heated by a d.c. arc, and are manufactured commerically in England as "Pointolites". These were calibrated over a range of brightness temperatures from 1800° to 3000°K by the use of an optical pyrometer and the tungsten emissivities of de Vos[11]. These sources are very stable and reproducible, and the calibration is accurate to within + 15°K. The effective brightness temperature of the image S' is calculated allowing for the measured light losses at L_1, B_1, and W_1. The filters F_1 and F_2 are a matched pair. Two pairs centered with the aid of a Hilger monochromator at 4272 Å and 5893 Å were used to isolate the Cr resonance triplet at 4254, 4271, 4289 Å, and the Na resonance doublet at 5890 and 5896 Å, respectively. These filters are made by Baird Atomic Inc., and have a pass band of around 45 Å and a transmission around 50%. The photomultipliers are EMI type 9558 having photocathode sensitivities of around 100μa/lumen. The current in each dynode chain was about 5 ma., which ensures a linear response to light intensity variations. The linearity was confirmed by inserting various calibrated neutral filters into the optical beams. The photomultiplier anode loads are 47KΩ, affording an over-all oscilloscope time-response of about 10μ sec.

Temperature Measured by Reversal Method- The temperature measured in a line reversal experiment is essentially the excitation temperature of the electronic state giving rise to the spectrum line concerned, and as such is defined by the Boltzmann relation in terms of the relative number of atoms in this state. This population will be sensitively determined by the balance between the collisional and radiative transfer processes leading to excitation and de-excitation. If the collisional processes involve the efficient transfer of energy from a degree of freedom which is slow in attaining thermal equilibrium (i.e. is relaxing), then the measured temperature will be the effective temperature of this degree of freedom. In this respect, there are many reasons for believing that the excitation temperature of the metallic atom used in reversal measurement is in equilibrium with the vibrational temperature of the gas. Evidence supporting this correspondence between the temperatures is given below.

It is unlikely that thermal excitation of an atom will occur efficiently on collision with another atomic species, since the energy and momentum transfer between a heavy atom and light electron is small. This is borne out by studies of quenching of resonance fluorescence of metallic vapours[12] and by reversal temperature measurements behind shock waves in inert gases containing metallic atoms[13]. The work of Ref. 12 indicates effectively zero quenching cross sections at low temperatures. The work of Ref. 13 indicates a weak coupling between translational and electronic energy at higher temperatures, which may arise from a radiationless transition at the elevated cross-over point of repulsive potential curves for the diatomic complex formed during the collision. The cross sections measured for this process are many orders less than the gas-kinetic values. For similar reasons, excitation by direct transfer of translational or rotational energy from a molecule to an atom can be precluded, rotational transfer being further unlikely on the basis of angular momentum conservation.

The quenching of resonance fluorescence of metallic atoms by molecules is, however, known to occur readily, and in some cases with almost every collision[14]. A theoretical examination of this process, such as given by Laidler[15], shows that during the lifetime of the collision complex there is a high probability that the electronic excitation of the atom will be converted to vibrational energy of the complex which, on separation, leaves the quenching molecule vibrationally excited. The work of Karl and Polanyi[16] indicates, as might be expected, that the quantum of electronic energy concerned appears initially in the nearest resonant vibrational level.

Previous line reversal measurements behind shocks in diatomic gases have shown that the reversal temperature changes with time in a manner clearly indicating that this temperature is in equilibrium with the relaxing vibrational temperature of the gas. For N_2 and CO, the temperature from Na and Cr reversal rises slowly at rates consistent with the vibrational relaxation times as measured independently by other workers using interferometry and infra-red emission techniques[17,18]. The results for N_2 are indicated in Fig. 4. Behind shock waves in O_2, CO_2 and H_2 the reversal temperature has been observed to fall at rates indicative of, and consistent with, the fall in vibrational temperature expected due to dissociation[17,19].

Thus, the evidence for the equivalence between measured reversal and vibrational temperature is unquestionably strong. The use of the method in the present work is advantageous since only relatively small amounts of vibrational energy are contained in the N_2 flows, but the effect of changes in this energy on the vibrational temperature is significant. Furthermore, since the intensity of spectral emission varies extremely rapidly with temperature (at 2500°K, the intensity in the blue region varies effectively as the 14th power of the temperature), the vibrational temperature can be measured to within a few percent.

2.3 Pressure Measurement

The measurement of static pressures in nozzle-flow studies of the present kind is desirable for two reasons. First, the static pressure is a basic gasdynamic variable whose measured distribution effectively defines and/or assesses the

actual fluid dynamics of the flow being studied. Confirmation of the basic thermo-gasdynamic environment is obviously necessary in order to employ with confidence more difficult or refined diagnostic techniques such as the spectroscopic line-reversal method previously described. Second, where the nonequilibrium process of interest involves sufficient enthalpy and the gas is sufficiently expanded, the measurement of static pressures can be a useful method (if not the only ready method) of detecting departures from equilibrium flow.

The present approach to the measurement of the flow static-pressure distribution has been to instrument the nozzle wall with flush-mounted transducers rather than attempt to develop static pressure probes for insertion into the flow as done by some previous workers (e.g., Ref. 6). Notwithstanding the more serious mechanical-shock problem encountered, this approach was followed because it presents essentially no problem whatsoever as regards basic interpretation of the measurement. That is, the measured pressure at the wall is the local flow static pressure. In contrast, in a nonequilibrium, supersonic or hypersonic nozzle flow characterized by large axial gradients the relation between static pressures measured on a probe to those which would exist in the absence of the probe poses a major research problem in itself. Not only the complex fluid dynamic, but equally important, the nonequilibrium character of the local flow field generated by the probe must be fully understood to interpret the probe measurement. Otherwise, probe nonequilibrium effects (initiated by the probe shock wave, say), which might well distort or mask those under study, could lead to serious misinterpretation. The calibration of such effects would appear exceedingly difficult, if not impossible.

In the present work, the nozzle-wall pressure transducer used is the Kistler piezoelectric transducer, model 401 (PZ-14). The piezoelectric element is quartz. The transducer has a sensitivity of 4$\mu\mu$cb/psi over the range of pressures calibrated, namely 0.1 to 3000 psi, and a natural-ring frequency of 50 Kc. The direct calibration of the transducer is by a dead-weight tester over the range 30 to 3000 psia. Below 30 psia, a simple dynamic calibration method is used. This entails exposing the transducer to a reservoir of gas at known pressure by means of a rapid-acting mechanical value. The calibrations are linear over the above pressure range and reproducible to better than 2% even after several months usage. As with any very high-impedance transducer, it is necessary to take particular precautions to avoid charge leakage due to dirt or moisture in order to obtain consistent performance.

Transducer response to normal acceleration of the nozzle wall occurring from mechanical shock is minimized by use of a relatively massive and soft mount having a low natural frequency. The ring frequency of the nozzle wall itself is made relatively high by appropriate structural design. The transducer is imbedded in a massive brass block which contacts the nozzle wall only through soft "O" rings (40 durometer). The stiffness of the mount can be varied by mechanical compression. To attain good spatial resolution and provide a combined heat sink and shield to minimize temperature effects, the transducer diaphragm is located a few thousandths of an inch behind an orifice in the nozzle wall. Orifice diameters range from about 1/16 to 1/8 inch, depending on the nozzle area ratio of the pressure station, and the orifice depth (i.e., local wall thickness) is about 1/32 inch. Adjustment of the orifice-cavity geometry was made until the response time of the system at any station was within the flow starting time.

In general, the performance of this transducer system has proved quite satisfactory. A further calibration check on the over-all transducer performance under conditions of nozzle flow is provided by the flow calibration experiments described in Sec. 2.4. The lower limit of measurable pressure is currently about 0.25 psi. This limit could probably be further reduced by additional improvement of the mechanical isolation.

2.4 Flow Calibration Experiments

Reservoir State - Measurements of the reservoir pressure attained behind reflected shock waves were made over a wide range of conditions with the PZ-14 pressure transducer. The purpose of these measurements was to determine the consistency with which the reservoir pressure could be measured with this transducer and to determine the agreement of the measured pressure with that calculated on the basis of the measured wave speed. The measurements were made for undertailored, tailored, and over-tailored shock-wave conditions using both hydrogen and helium driver gases. In general, the measured reservoir pressures were found to agree to within about 5% with the calculated pressures immediately behind the reflected shock wave.

In order to check the calculated reservoir temperatures, several temperature measurements were made using the line-reversal method behind reflected shocks in N_2 (see also Sec. 3.2). These measured temperatures, which were restricted to below 3000°K by the upper limit imposed by the background reversal source, were in good agreement with the theoretical equilibrium values calculated from the measured wave speed. Above 3000°K, the measured reservoir pressures agreed well with those calculated from the measured wave speed, as noted above. This agreement of pressures lends some confidence to the use of calculated reservoir temperatures above 3000°K.

In order to determine whether the opening of the nozzle diaphragm produced any significant effect on the reservoir temperature, several line-reversal measurements were made with normal diaphragm rupture and with the nozzle entrance blanked-off completely. No difference in the measured temperatures was observed.

Nozzle-Flow Calibration - A large number of calibration experiments were conducted in the conical nozzle to determine the reliability of the pressure measurement techniques and establish the effects of wall boundary layer. In order to eliminate real-gas effects and cover a wide range of flow conditions, static pressure distributions were measured for test-gas flows of helium, nitrogen, and argon at reservoir temperatures and pressures of 300°K and 15 atm., 2000°K and 60 atm., and 4000°K and 120 atm., respectively. For the

nitrogen calibration flows, vibrational excitation was small with consequent very small effect of vibrational relaxation on pressure. The shock-mount stiffness and orifice-cavity geometry of the pressure transducers were adjusted during these studies to minimize acceleration response and obtain response times (200μ sec.) less than the nozzle starting times. For each gas used in these flow calibration studies, the pressure data indicated a scatter within ± 5% of the mean value of the pressure observed at each nozzle station. In addition, the data indicated monatonically decreasing pressures with increasing area ratio. The experimental pressures, however, were higher than values calculated for pseudo-one-dimensional, inviscid flow. The difference between the measured and calculated pressure distributions was attributed to nozzle wall boundary layer.

For the helium-flow calibration studies (T_o = 300°K and P_o = 15 atm.), relatively large differences between the measured and inviscid pressure distributions were observed. These large differences were interpreted as due to a turbulent boundary layer which, in this case, was made relatively thick by the lack of boundary layer cooling (i.e. near adiabatic-wall condition). For the argon-flow studies, on the other hand, a highly cooled boundary layer (T_w/T_o = .075) coupled with high reservoir pressures resulted in small deviations of the observed pressures from the inviscid values. In total, the pressure data from these calibration experiments provided a good means for evaluating a theoretical correction to the nozzle area ratio to account for boundary-layer displacement. For this purpose, the pressure distributions calculated from inviscid, pseudo-one-dimensional (or source-flow) theory were corrected for boundary-layer displacement as described below, and compared with the experimental data. The assumption of source flow for the inviscid-flow model is a very good approximation for the present nozzle geometry.

For the range of Reynolds numbers involved in the calibration experiments as well as those of Secs. 3 and 4, the nozzle wall boundary layer was assumed to be turbulent. The existence of turbulent boundary layers was also verified directly by the measurement of nozzle-wall heat-transfer rates using thin-film heat transfer gages. The displacement thickness δ^* was calculated from a semi-empirical formula after Burke[30] who examined the approach of local similarity as well as equivalent flat plate flow. The particular expression used in the present work is

$$\frac{\delta^*}{x} = 0.104\left(1+\frac{\gamma-1}{2}M^2\right)\left(1+1.5\frac{T_w}{T_o}\right)\left(\frac{\gamma-1}{\delta}\right)^{\frac{1+\omega-m}{m}}\frac{(M^2)^{\frac{1+\omega}{m}}}{Re_x^{1/m}}$$

where ω is the exponent in the viscosity law $\mu \sim T^{\omega}$, $m = 3$, Re_x is the local stream Reynolds number based on x, M is the local Mach number, and x is distance from the throat where δ^* is taken to be zero. It may be noted that, apart from the present calibration experiments, this expression has previously been tested with a variety of experimental data[30] and shown to be accurate over the present range of Mach numbers. In all of the present experiments the ratio δ^*/x did not vary strongly and was of order .01.

Over the entire range of calibration experiments, agreement to within a few percent was generally obtained between the measured pressure distributions and those calculated by applying the above displacement thickness to reduce the inviscid-flow area ratios. An exception to this generally good agreement was observed at an area ratio of 4, as discussed in Sec. 4.1. In order to illustrate typical results, calibration data for the nitrogen experiments are shown in Fig. 3. A typical oscilloscope record of the transducer response is shown in the upper right corner of this figure. The horizontal separation of the two theoretical curves indicates the effect of the wall boundary layer on the nozzle area ratio. The two sets of experimental pressure data indicate the typical agreement with the corrected theory, as well as the reliability of the pressure instrumentation. Similar agreement obtained in all calibration experiments permitted a confident assessment of boundary layer effects in the nonequilibrium flow experiments to be described, particularly those in Sec. 4.

Nozzle-Flow Test Time - The spectrum-line reversal method has the additional advantage of clearly indicating the termination of the nozzle test time, as determined by the arrival of the driven-driver gas interface in the nozzle. The interface is revealed by a fall-off in light emission and temperature, as indicated in the typical record shown in Fig. 5. In all the observations, over a wide range of reservoir conditions, the test time was much less than that expected even allowing for the usual reduction due to real-gas and non-ideal flow effects. Operation with H_2 as the driver gas at tailored-interface conditions gave no noticeable improvement in test-time. The testing times using He as the driver gas at very much over-tailored conditions were longer than those obtained with H_2 driver at the tailored condition.

These observations were further confirmed by the previously mentioned temperature measurements made in the reservoir region behind the reflected shock. The observations made in this region with and without the nozzle operating further showed that the duration of test time was not significantly influenced by the mass outflow through the nozzle. In both the reservoir region and in the nozzle, the interface arrival as detected by thin-film resistance thermometers corroborated that indicated by the line reversal measurements.

The observed flow test times were about one-half and one millisecond, respectively, for the N_2- and H_2-flow experiments to be described in Secs. 3 and 4. These observed test times were of the order of one quarter those calculated for ideal flow.

3. NITROGEN VIBRATION STUDIES

Previous studies of the efficiency of de-excitation of N_2 vibration by nitrogen molecules have been confined to measurements made behind incident shock waves[9, 10], or in other systems where vibrational energy relaxes towards a final equilibrium state under the dominant influence of the excitation process[31, 32]. The relaxation times inferred from these measurements are plotted in Fig. 4 versus the final equilibrium temperature attained. The normal-shock measurements were all made during the final stages of the relaxation, where the extent of the departure from equilibrium is relatively small and the Landau-Teller

theory[9, 20] is therefore expected to be valid.

It has been assumed to date that the de-excitation rates inferred from the normal-shock studies can be used with the Landau-Teller theory to calculate the vibrational lag in nozzle expansions (see, for example, Ref. 5). Calculations based on these assumptions predict substantial freezing of vibrational energy in the expanding-gas flow, which could produce a significant reduction in the available free-stream enthalpy. However, as previously noted in the introduction, the present measurements of vibrational temperatures discussed in Secs. 3.1 and 3.2 indicate that the vibrational energy remains much closer to equilibrium in the nozzle expansions than such calculations predict. The interpretation of this significant result is discussed in Sec. 3.3.

3.1 Evaluation of Vibrational Temperature

A typical oscilloscope record of Na-line reversal obtained in the expansion of N_2 is shown in Fig. 5. The upper trace shows the emission signal as recorded by P_2 (see Fig. 2), and the lower trace the absorption as recorded by P_1 against the background source S_1 at an effective brightness temperature T_{B_1} = 2160°K. (Since the other source S_2 is not operating, its effective background temperature, T_{B_2}, is that of the room - i.e. T_{B_2} = 300°K.) Due to the very low vibrational temperature in this particular expansion the emission beam was operated at a much higher amplification than the absorption beam. Since the beams are balanced at equal sensitivity, the true amplitudes of these signals are obtained from a known scaling factor.

In this record, if the true signal amplitudes are respectively e and a units of emission and absorption, and the observed excitation temperature of the Na is T_v, then we may write, using Wien's approximation to Planck's Law

$$e = k_e \varepsilon_\lambda \exp(-C_2/\lambda T_v)$$

$$a = k_a \left[\exp(-C_2/\lambda T_{B_1}) - (1-\alpha_\lambda)\exp(-C_2/\lambda T_{B_1}) - \varepsilon_\lambda \exp(-C_2/\lambda T_v)\right]$$

In these expressions, k_e, a are constants which depend on the optical and electronic properties of the beams, the shape of the spectrum line used and the density of the Na atoms. These constants are made equal for each of the two beams by the optical arrangement and the initial balancing procedure, described in Sec. 2.2. ε_λ and α_λ are respectively the emissivity and absorptivity of the gas at the wavelength λ concerned, and C_2 is the second radiation constant. In the expression for a, the first term represents the steady d.c. light level from the background as represented by the oscilloscope trace prior to the arrival of the expanding gases, the second term the transmitted intensity after absorption of this light at the Na wavelength, and the third the Na emission from the expanded gases.

From the above relations, and using Kirchoff's Law which states the equality between spectral emissivity and absorptivity,

$$\exp(-C_2/\lambda T_v) = \left(\frac{1}{1+a/e}\right)\exp(-C_2/\lambda T_{B_1})$$

From this expression, with the knowledge of T_{B_1} and a measurement of the signal amplitudes at various times during the flow of expanded gas, the temporal behavior of the vibrational temperature T_v may be evaluated simply and quickly. The evaluation of T_v for the record shown in Fig. 5 is given in the lower half of this figure. Two features are worthy of special note in these oscilloscope records and their temperature analysis.

First, although the amplitude of the oscilloscope signals depends on both the local temperature and the concentration of metallic atoms, the method of measurement is able to discriminate between variations in these two quantities. For example, if the concentration increases, both signals increase in amplitude but their ratio remains the same, so that the measured temperature does not vary. If the temperature increases, the emission also increases but the absorption decreases, and vice versa. Thus, it is noted in Fig. 5 that the large change in signals beginning at about 0.3 msec. is actually due to a density increase.

The second feature to be noted is that the large fall in emission at the start of the flow actually represents only a relatively small decrease in temperature. In fact, a decrease in temperature of only 100° at 2000°K will almost halve the emission amplitude at the Na wavelength, and more than halve it at the Cr wavelength. This feature affords a very precise determination of the temperature. The amplitudes of the oscilloscope signals may be easily read to within ± 10%, and this represents an error of only ± 10°K at 2000°K. The background source is calibrated to within ± 15°K, so that the over-all error is certainly within ±30°K. Thus, the error in temperature measurement is less than ± 2% for the temperature range considered in the present work.

This measureable temperature range in the present application extends from 1500° to 3000°K. The lower limit is set by the noise level arising from statistical fluctuations at the photocathode surfaces. The upper limit is determined by the melting point of the tungsten "Pointolite". The lower limit in the present work corresponds to an improvement of more than an order of magnitude in sensitivity over that of previous work[21].

Introduction of Na and Cr - In the present experiments, temperature measurements were made using both Na and Cr as reversal elements. The Na was introduced by passing the N_2 test gas into the shock tube over a heated spiral filament of platinum, previously coated with NaCl. This method has been used successfully in previous work[21], and gives a uniform and reproducible suspension of NaCl smoke particles in the test gas. The Cr was introduced by mixing small amounts of the volatile compound $Cr(CO)_6$ with the test gas

prior to filling the tube. Partial pressures of 0.1% or less of $Cr(CO)_6$, and trace amounts of NaCl were used. In each of these cases, the added compound has been previously observed[13] to dissociate rapidly in the primary shock front, the amount of heat involved in the process being exceedingly small.

3.2 Experimental Results

Initial Observations - The results of the initial measurements of N_2 vibrational temperatures at area ratios of 8 and 32 in the conical nozzle are shown in Fig. 6. The two experimental temperatures shown represent the superimposed results of many consistent observations for expansions from conditions of a constant reservoir temperature, T_0, of 4500°K and a constant reservoir pressure, P_0, of 50 atm. In these initial experiments, Cr was used as the line-reversal element. In additional experiments, described later in this section, similar observations were made using Na. The results of many of these Na observations at the area ratio of 8 are also shown by the superimposed point in Fig. 6. It is noted that the vibrational temperatures measured with each element coincide almost exactly. The significance of this feature is discussed later in this section. The experimental points shown have not been corrected for the change in area ratio due to the boundary layer since the corrections involved in this case are rather unimportant (see Fig. 3).

The upper curve in Fig. 6 represents the vibrational temperature distribution in the nozzle as calculated by the use of the Landau-Teller theory, using the vibrational relaxation times τ_6 for N_2 as given by the shock-tube data of Fig. 4. This method of calculation is described briefly below and in detail in the appendix. The lower curve in Fig. 6 is the vibrational temperature distribution for equilibrium flow, that is, for $\tau_s = 0$ or zero relaxation time.

It is seen in this figure that the observed vibrational temperatures lie much closer to equilibrium than predicted by the use of Landau-Teller theory.

In view of the large discrepancy between the measured and calculated vibrational temperatures a series of crucial additional experiments were carried out to substantiate the validity of the above temperature observations. These experiments are described below.

Additional Experiments - These consisted of

(i) measuring the reservoir temperature behind the reflected shock with the same optical line-reversal system, and similar conditions of temperature and pressure as in the nozzle.

(ii) varying the amount of metallic additive ($Cr(CO)_6$) over a wide range, and observing if any changes occurred in the measured temperatures.

(iii) making temperature observations with Na in addition to Cr additive.

The reservoir temperature measurements were made in the range 2000-3000°K, and the observed temperatures agreed well with those predicted from the wave speed and reservoir pressure measurements. At the lower measured temperatures, the vibrational relaxation immediately behind the reflected shock was revealed by an initially low and subsequently rising reversal temperature, as in previous work[17]. This series of experiments confirmed the ability of the present technique to measure temperature accurately under conditions similar to those in the nozzle.

Varying the amounts of Cr additive served to reveal three possible effects. The first and most obvious was the determination of whether the additives were themselves affecting the temperature, either directly by absorbing enthalpy in their decomposition, or indirectly by acting as impurities in the relaxation process. The second was concerned with the possibility that the metallic atoms, by virtue of the efficient coupling of their electronic excitation with the N_2 vibrational energy, were effectively radiating vibrational energy from the system. The third was whether the presence of colder metallic atoms in the denser gas of the nozzle boundary layer was spectroscopically masking the reversal measurements. Each of these effects would cause the measured temperatures to be too low.

In these experiments, the $Cr(CO)_6$ concentration was varied from 10^{-1}% to 3×10^{-3}% by pressure for constant reservoir conditions. No change in the measured vibrational temperature was observed, and it was concluded that the above three effects were unimportant. As regards the boundary layer, any effect here would have resulted in an increase in measured temperature as the $Cr(CO)_6$ concentration was decreased over this wide range.

It is of interest to note that throughout the course of this work, check experiments were repeated wherein no Na or Cr additives were used. In these cases, no light emission or absorption was observed. This confirmed that the source of the radiation was due to the Na or Cr atoms, and not to any extraneous effects.

The temperature measurements made in the nozzle using Na as well as Cr as the additive were carried out for similar expansion conditions. The measured temperatures for both Na and Cr were in complete agreement (see Fig. 6). This result bears significantly on the following more serious question. If the exchange of vibrational quanta between levels is not as efficient as predicted theoretically (see appendix), the possibility of a non-Boltzmann distribution in vibrational energy arises during the expansion. This distribution would not then be characterized by a single vibrational temperature, since each level would have its own effective excitation temperature as determined by its population. Since the Cr resonance states lie closest to the 11th, and the Na resonance states closest to the 7th vibrational levels of N_2, a non-Boltzmann distribution would be revealed by differing line-reversal temperatures for these metals. This was not observed, and it therefore appears that a Boltzmann distribution between the vibrational levels existed during the expansion.

The results of these additional experiments gave no reasons to doubt the validity of the vibrational temperatures measured by line-reversal in the present work. Indeed, the results of all the additional experiments fully support the initial observations shown in Fig. 6.

Calculated Vibrational Temperatures - It was felt that the real disagreement between the calculated and measured temperatures gave cause for a re-examination of the method of calculation. The initial calculations of the vibrational distribution were based on a previous method[5] pertaining to the relaxation of vibrational energy under nozzle-expansion conditions. The method assumes the applicability of the macroscopic, Landau-Teller equation for vibrational relaxation under these conditions. As an alternative approach, we examined the behavior of the vibrational temperature from a microscopic viewpoint, i.e. in terms of the individual collisional processes of energy transfer and the probabilities of vibrational de-excitation, simplified by reasonable approximations and assumptions. The salient features of these two methods of calculation are outlined in the appendix. It is noted here that the microscopic formulation yields the macroscopic relaxation equation when the transition probabilities are assumed proportional to the quantum number of the upper vibrational level involved.

When applied to the expansion conditions of Fig. 6, as described in the appendix, the two methods predicted essentially the same vibrational temperature distribution; namely, that indicated by the upper curve of Fig. 6. Vibrational temperature distributions were then calculated for these expansion conditions using relaxation times which were effectively 10, 15 and 20 times shorter than those used in the upper curve. These distributions are also shown in Fig. 6. It is seen that the observed vibrational temperatures agree well with the distribution calculated for relaxation times which are 1/15 those inferred from the normal-shock studies.

Observations at Varied Reservoir Conditions - In view of the apparently much shorter vibrational relaxation times indicated by the initial observations, the experimental program was next extended to examine the behavior of the measured vibrational temperatures under various conditions of nozzle-flow pressure and temperature. Accordingly, two series of experiments were carried out.

The first series was conducted at a constant value of T_o = 4500°K, and P_o was varied from 24 to 82 atm. The second series of experiments was made at a constant value of P_o = 735 psi (50 atm.), and T_o was varied from 2800° to 4600°K. The vibrational temperatures observed in these two experiments are shown in Figs. 7 and 8, respectively. The full curves in these figures represent the vibrational temperatures calculated (as indicated in the previous sub-section) on the basis of a relaxation time again 15 times shorter than that inferred from normal-shock studies. The portions of broken curves indicate the vibrational temperature calculated in the same way, but using relaxation times 10 and 20 times shorter. Two main features are immediately apparent from these figures.

First, in Fig. 7 the difference of about 150°K between the measured vibrational temperatures at the two area ratios 8 and 32 clearly shows that the vibrational energy is not totally frozen at these stages in the expansion.

Second, in both Figs. 7 and 8 the comparison between the experimental points and the calculated vibrational temperatures based on shorter relaxation times strongly supports the interpretation of the data in terms of a much faster relaxation of vibrational energy under the present expansion conditions. Although there is some suggestion of a departure at low temperatures and pressure, the consistent trend of agreement between the measured vibrational temperatures and the curve calculated on the basis of a relaxation time 15 times shorter is to be noted. This general trend is evident not only over the wide ranges of temperature and pressure, but also at the two area ratios used in the experiments. It clearly indicates that, under the present expansion conditions, the N_2 relaxes at an apparent rate about 15 times faster than under normal-shock conditions.

3.3 Discussion of Results

Considerable care has been taken in confirming the validity and interpretation of the spectroscopic studies of vibrational relaxation described in the previous section. Other potential grounds for questioning their validity have been explored and invalidated. Mention will be made of these before proceeding to discuss the significance of the main results.

In the above measurements by spectrum-line reversal, it is recognized that fictitiously low reversal (vibrational) temperatures could be obtained if the Na or Cr electronic excitation were not in radiative equilibrium, or if this excitation were unduly quenched by the transfer of electronic energy to the N_2 translational degree of freedom. However, in the former case, for even the least favorable conditions of nozzle pressure and temperature, the rate of population of the electronic levels by vibrational transfer was always significantly greater than their rate of depopulation by radiation. Thus, any departures from electronic equilibrium by radiative depletion of these levels would have been insignificant. In the second case, quenching by the translational degree of freedom could, at most, increase the rate of electronic depopulation by a factor of two, and this would result in an effective reduction in reversal temperature of only 100°K. On the basis of the results of previous work[17] and the arguments given in Sec. 2.2, such a process, however, would be unlikely to occur. Furthermore, the identical reversal temperatures recorded by both Na and Cr made the occurrence of both of the above mechanisms even more remote.

The effect of impurities, such as water, on the rate of relaxation is not considered important in the present work. The total impurity content of the N_2 gas used was less than 100 ppm. Further, in the present expansion flows impurities would be expected to be less important than in normal shock-wave flows. The reason for this is that, under the present conditions, the impurities would be initially dissociated behind the reflected shock and would thus not be present as molecular species in the initial expansion process.

Any impurity effect due to the liberation of CO in the decomposition of the $Cr(CO)_6$ additive would have been revealed in the experiments in which the percentage of this additive was varied over a wide range. Thus, the possibility of an effective de-excitation of N_2 vibration by way of the exchange of vibrational energy with CO molecules, and the subsequent radiative de-excitation of these species, is

excluded. The relatively long radiative lifetime of the vibrationally-excited CO molecules would further disfavour this process.

Two remaining possible sources of error are the balance in the sensitivity of the two line-reversal beams and the calibration of the background lamps. Serious errors from these sources, however, are hardly conceivable. The sensitivity of the two beams would have to be in error by two orders to explain the discrepancies in the vibrational temperatures. Similarly, the measurements of the brightness temperatures of the background sources would have to be in error by almost 1000°K.

We have thus been unable to find grounds on which to doubt the measured temperatures, or their interpretation in terms of the vibrational temperature of the expanding gas. In the latter respect, it is illustrative to note that for the particular expansion conditions and area ratio at which the typical temperature record shown in Fig. 5 was obtained, the equilibrated translational and rotational temperature was only 800°K. This temperature is well below the value of 1570°K measured from this particular record; the intensity of Na radiation at 800°K is less than that at 1570°K by a factor of 3×10^6. The only existing excitation mechanism in the expansion having sufficient energy to produce this observed degree of electronic excitation is via the interchange of vibrational to electronic energy.

It is concluded that the results of the present work, when interpreted on the basis of the Landau-Teller theory of vibrational relaxation, indicate that the probability of vibrational de-excitation under the present nozzle-flow conditions was significantly greater than that obtained under normal-shock conditions. However, we consider that this in no way reflects on the results of the normal-shock studies, but rather that the application of these results to the present nozzle-expansion conditions must be questioned. Certainly, one would not expect measurements made by the same method -- i.e. line-reversal -- in the two non-equilibrium systems to produce widely differing results if the two systems were not, for some reason, incompatible.

In normal shock wave studies, the rate measurements are made principally during the final approach to equilibrium. The fact that the Landau-Teller theory apparently predicts vibrational relaxation reasonably well in this region does not necessarily imply that it would do so over the entire relaxation range where the departures from equilibrium are much more severe. It would be surprising if it did, since it specifically deals with relatively small departures from equilibrium wherein the translational temperature is not changing greatly. As previously noted, in nozzle flows the departures from equilibrium are such as to produce vibrational temperatures much in excess of the translational temperature, the opposite situation to the normal shock wave. Under nozzle-expansion conditions, the different nature of the collisional processes may conceivably be such as to render the Landau-Teller assumptions of de-excitation invalid. The relation between the de-excitation probabilities for the individual vibrational levels, as discussed in the appendix, may differ from the simple numerical type proposed by Zener[22] on the basis of his model of molecular interaction. A small dependence of de-excitation probability on the vibrational as well as translational energy of the colliding partners might significantly affect the nozzle-flow relaxation processes. In the normal shock wave, where the temperatures are comparable in the observed relaxation regions, such an effect might not be revealed.

Cottrell and McCoubrey[24], in discussing vibrational energy transfer, indicate possible errors in estimates of de-excitation probabilities which they review. We have investigated these in relation to the present work, but they offer no explanation. However, these authors do raise an interesting point concerned with a fundamental difference between excitation and de-excitation processes which may have some bearing. Due to attractive forces between molecules, there exists a finite probability of de-excitation even at zero temperature when, of course, the excitation probability is zero. In this light, it may be reasonable to attach to the de-excitation probability some dependence on the vibrational temperature.

In a recent paper, Bauer and Tsang[33] point out several chemical mechanisms hitherto overlooked which at high temperatures can make vibrational relaxation much faster than expected from the usual inelastic collision theory. These mechanisms equilibrate translational and vibrational energies through chemical exchange reactions where, for example, atomic partners in a collision of two diatomic molecules could be interchanged. On the basis of the estimates given by these authors, however, the temperature range of the present experiments appears too low for these mechanisms to be significant.

It is not considered that the faster rates of vibrational relaxation inferred from the present work have any direct implication concerning the applicability of atomic recombination rates inferred from shock-wave dissociation studies to nozzle flows of dissociated gases. Vibrational de-excitation is essentially a two-body process, and its efficiency is determined to a large extent by the relative velocity (i.e. kinetic temperature) of the two colliding molecules. On the other hand, recombination is essentially a three-body process and exhibits only slight dependence on temperature. However, the present work may reflect indirectly on the behavior of expanded flows of dissociated gases. In such flows, the vibrational temperature is ultimately determined by the balance between the rate of population of vibrational levels due to atomic recombination into these levels, and the rate of depopulation due to the transfer of energy from the vibrational to the translational degrees of freedom. An enhancement in the rate of the latter process may therefore affect the rate of recombination via its intermediate coupling with the vibrational temperature.

4. HYDROGEN RECOMBINATION STUDIES

Molecular dissociation, in contrast to molecular vibration, can involve large amounts of energy and as such can exert a significant influence on the thermo-gasdynamic characteristics of flow systems[2-4, 25]. For highly dissociated flows of current interest, such as the re-entry flows about

hypervelocity bodies and various internal flows as in high-temperature shock tunnels and rocket nozzles, the extent of nonequilibrium between dissociation and translational degrees of freedom must therefore be considered. As a result, a great deal of effort has been expended in recent years to obtain appropriate high-temperature chemical rate data in shock-tube experiments (eg. Refs. 26-28). These experiments entail study of the flow behind normal shock waves where molecular dissociation is the dominant process in the approach to the final equilibrium state attained. Recombination-rate constants appropriate to expansion flows as in rocket nozzles are inferred from such shock-tube measurements by assuming that the equilibrium mass-action law is valid for nonequilibrium conditions, and that the shock-wave kinetic data can be extrapolated to the nozzle flow where the thermo-gasdynamic environment is very different.

There is a need to verify the extrapolation of shock-wave chemical rate data to expansion flows, as well as obtain improved values of recombination rate constants at high temperatures. This need is particularly evident as regards the use of hydrogen as a high-temperature rocket propellant. Theoretical estimates of hydrogen rocket performance show that small changes in the frozen atom concentration can result in significant changes in specific impulse[25]. The technical importance of the dissociation-recombination kinetics of hydrogen is evidenced by the recent research emphasis on dissociated H_2 flows[7,26-28]. While this interest in H_2 stems mainly from its potential as a rocket propellant, the kinetics involved also have a fundamental significance as regards expansions of dissociated air about re-entry bodies. Despite the recent emphasis on H_2 kinetics, it may be noted that the hydrogen-atom recombination rates inferred by various investigators from shock-wave dissociation studies[26-28] vary by as much as a factor of six. This situation is in contrast to that for nitrogen vibration, previously discussed, where the shock-wave rate data of different investigators are generally in good agreement (cf. Fig. 4).

In the present studies, a mixture of dissociated hydrogen and argon was expanded in the 15° conical nozzle from an equilibrium reservoir temperature of 6000°K over a range of reservoir pressures from 28 to 112 atm. Wall static pressure distributions were measured. The purpose of the experiments was twofold: first, to reveal any departure of static pressures from the limiting values for chemical equilibrium; and second, to interpret observed departures from equilibrium pressures in terms of hydrogen-atom recombination rates.

A basic difficulty arises in attempting to infer chemical reaction rates from measured static pressures in such flows. The static pressure is inherently rather insensitive to the flow chemistry. As a consequence, the accuracy of pressure measurement necessary to determine a rate to better than a factor of two is difficult to attain, exceedingly so in the present type of nozzle-flow experiment employing shock-tube methods. While the accuracy of pressure measurement can be made much higher in steady-state nozzle-flow systems, the shock-tube approach is unique in providing the high reservoir temperatures of present interest, as well as high chemical purity. Notwithstanding their limited usefulness in determining reaction rates, the present experiments were considered a necessary prelude to the development of special diagnostic techniques more sensitive to the H_2 nozzle-flow chemistry.

The use of argon as an inert diluent for hydrogen in the present studies was necessary in order to attain the desired high reservoir temperature by dependable shock-tube driver techniques. Also, the use of argon facilitated comparison of rate constants with results from various shock-wave dissociation studies made with H_2-Ar mixtures. Calculations indicated that an undissociated test-gas mixture containing about 8% H_2 would give a large amount of enthalpy in dissociation relative to the total enthalpy at the reservoir conditions of interest. A large amount of energy in dissociation was necessary in order to expect measureable effects of chemical nonequilibrium on the nozzle-flow static pressures. A premixed cylinder of H_2-Ar test gas for the experiments was obtained from the Matheson Co. Inc. of East Rutherford, New Jersey. The analysis of this mixture, furnished by the supplier, gave the following composition:

H_2 -- 7.95%
Hydrocarbons -- less than 100 ppm
N_2 -- less than 100 ppm
Argon -- Balance

At the equilibrium reservoir conditions attained behind the reflected shock wave, i.e. 6000°K in temperature and 28 to 112 atm. in pressure, the hydrogen was more than 90% dissociated in all cases. Because of this high level of dissociation, and also the high natural frequency of H_2 vibration, the reservoir energy in molecular vibration was very small relative to that in dissociation. Thus, from the viewpoint of the energy involved, a lag in hydrogen atom recombination was expected to be the dominant nonequilibrium process in these expansions. Observed departures from equilibrium could then be reasonably attributed to this cause alone.

4.1 Experimental Results

The initial experiments with the H_2-Ar mixture were carried out at equilibrium reservoir conditions of 6000°K temperature and 57 atm. pressure. The reservoir conditions attained behind the reflected shock wave were determined by calculation from the measured speed of the incident shock-wave and the initial test gas conditions. In each experiment the reservoir pressure was also measured. Wall static pressures were measured at nozzle area ratios A/A^* of 4, 8, 16, 32, and 64 using the techniques described in Sec. 2.3. These geometric area ratios were corrected for wall boundary-layer displacement using the expression for δ^*/x previously given in Sec. 2.4.

The range of stream Reynolds numbers Re_x in these experiments was approximately $.5 \times 10^6$ to 2×10^6. The assumption of a turbulent wall boundary layer on which the present expression for δ^*/x is based was verified by thin-film measurement of wall heat-transfer distributions. These heat transfer studies were made in a 15° wedge nozzle with the same H_2-Ar mixture and reservoir conditions as employed in the present conical nozzle studies. In the present experiments the local displacement thickness was less than 10% of the nozzle diameter. The corrections

to the geometric nozzle area ratios were obtained by evaluating δ^*/x for local equilibrium-flow values of M and Re_x. On the basis of the inviscid-flow calculations for finite reaction rates to be discussed in Sec. 4.2, the effect of chemical nonequilibrium on δ^*/x was found to be negligible. In evaluating Re_x, the viscosity μ was taken to be that for pure argon.

Typical measured pressure distributions from the initial experiments at 57 atm. reservoir pressure are compared in Fig. 9 with the calculated limits for chemically frozen and equilibrium inviscid (source) flow. The geometric, nozzle area ratios at which the pressure data were obtained have been corrected, as described, to account for wall boundary-layer displacement.

The measured static pressures shown in Fig. 9 are seen to lie below the limit for equilibrium chemistry but above that for completely frozen chemistry. It may be noted that in this case the corrections to the geometric area ratios to account for boundary layer are rather small, and that the experimental data indicate lower than equilibrium pressures even without such corrections. The maximum scatter in the data occurs at the lowest pressure level and is somewhat less than $\pm$ 10% of the corresponding mean value. The average scatter in the data, however, is only about $\pm$ 5%. The reduction in observed pressure from the calculated equilibrium limit is considered to be a real effect, not in doubt on account of either data scatter or boundary layer effect. This pressure reduction is interpreted as evidence of a lag in hydrogen-atom recombination occurring in the flow expansion process.

Subsequent to the initial experiments at 57 atm. reservoir pressure, additional pressure measurements were made for reservoir pressures of 28 and 112 atm. at the same reservoir temperature of 6000°K. A plot of all the measured pressure data, corrected for boundary layer, is shown in Fig. 10 along with the calculated limits for equilibrium and frozen flow for 57 atm. The calculated limiting curves are essentially independent of reservoir pressure over the range covered.

The measured pressure data of Fig. 10 generally show increased reduction from the equilibrium limit with decreased reservoir pressure. This general trend is as expected on the basis of (lagging) recombination of hydrogen atoms occurring via three-body collisions. Three-body recombination has a stronger dependence on pressure (density) by one order than has a two-body collision process such as dissociation. The experimental data of Fig. 10 for the lowest reservoir pressure of 28 atm. are seen to lie close to the calculated frozen limit, while those for the highest reservoir pressure of 112 atm. lie close to the equilibrium limit.

While the general trend and consistency of the pressure data in Fig. 10 is clear, two detailed features which are not understood should be noted. First, at the highest measured pressures where the corrected area ratio is slightly less than 4, the data cluster together for all reservoir pressures rather than showing the separation present elsewhere. Second, at the highest reservoir pressure of 112 atm. the experimental data at the two largest area ratios tend to lie slightly higher than the calculated equilibrium limit. These two features have been found to be quite reproducible. Although it is not considered that either of the effects influence the general interpretation made of the data (i.e. as reflecting recombination lag), we do not have a satisfactory explanation for their occurrence. The data cluster at area ratio 4 is the more serious effect. We are inclined to discount these particular data completely in view of slight discrepancies observed at the same area ratio in the nozzle calibration experiments described in Sec. 2.4, as evident in Fig. 3.

4.2 Comparison With Finite-Rate Calculations

The experimental data were considered sufficiently accurate to warrant comparison with calculated pressure distributions for the purpose of inferring recombination rate constants. The case of 57 atm. reservoir pressure was chosen for detailed comparison. Calculations of the inviscid expansion flow for finite reaction rates and the particular geometry of the 15° conical nozzle were carried out numerically using an existing IBM machine code previously developed at CAL (Ref. 4). Within the framework of the assumed kinetics, and pseudo-one-dimensional (or source) flow without transport phenomena, this code provides an exact numerical solution to the nonequilibrium flow. The initial conditions for starting the calculations were generally taken to be equilibrium conditions existing at the nozzle throat. This simplification was made to minimize machine computing times and had negligible effect on the solutions obtained.

The reaction mechanism assumed in these calculations was the complete dissociation-recombination reaction

$$H_2 + X \underset{k_r}{\overset{k_d}{\rightleftharpoons}} 2H + X$$

where X is any of the bodies Ar, H, or H_2. In the machine computing program, the forward and reverse rate constants, k_d and k_r, are related in the usual way through the equilibrium constant. In the first series of calculations carried out, the values of k_r corresponding to the various third bodies were taken to be constant, independent of temperature. Values of k_r approximately corresponding to the smallest values inferred in previous shock-wave dissociation studies with H_2-Ar mixtures[26-28] gave the calculated lower curve I shown in Fig. 11. This curve is seen to correspond approximately to the lower limit of scatter of the experimental pressure data. The magnitudes of the recombination rates were then increased by a factor of six to obtain the calculated upper curve II in Fig. 11, which lies approximately 10% above curve I.

It is noted that the above factor of six approximately corresponds to the range of variation in recombination rates inferred from shock-wave dissociation studies (with H_2 + Ar) by various investigators[26-28]. Further, the 10% difference in pressure between curves I and II produced by this factor of six change in rates represents the average scatter of the present data.

The particular values of the (shock-wave) rate constants employed to obtain curves I and II

are also tabulated in Fig. 11. It will be noted that the dominant rate constant in these calculations is that for the hydrogen atom as the third body. This rate constant is sufficiently large, that, despite the relatively low concentration of H as compared to Ar, the actual rate of atom recombination due to H as a third body considerably exceeds that due to Ar as a third body. The difference in pressure between curves I and II is thus largely due to the corresponding change in k_ℓ for H as the third body. This difference would not be strongly affected by changes of a different magnitude in k_ℓ for Ar and H_2 as third bodies. The hydrogen molecule, in particular, is relatively unimportant as a third body because of its very low concentration.

The fact that a change of a factor of six in rate constants produces a change in the calculated pressures of only about 10% illustrates the insensitivity of pressure to the flow chemistry and the basic difficulty of inferring rate constants from the pressure data. Taking the average scatter of the experimental data to be $\pm$ 5%, the best estimates of recombination rates to be inferred from the data of Fig. 11 are the geometric mean values of the rates shown for curves I and II. The uncertainty in these mean values is then a factor of about 2.5. It will be noted that these mean values lie within the range of variation of reported shock-wave results, as mentioned above. Within a factor of about 2.5, any incompatibility in the application of shock-wave rate data to the present expansion flows (i.e. analogous to what is observed for nitrogen vibration) would be masked not only by the scatter of the present data but also by the variation in the shock-wave results.

The difficulty of determining a unique recombination-rate constant from such pressure data is further illustrated by a second series of calculations carried out to reveal the effect of a temperature dependence of k_ℓ . Figure 12 shows typical results for the calculated pressure distributions. The lower curve is identical to curve I of Fig. 11. The upper curve was calculated assuming all k_ℓ values to be proportional to T^{-1} and matching with the k_ℓ values for the lower curve at the nozzle throat ($T \simeq 4500°K$). The slight difference between these two curves indicates that theoretical pressure distributions calculated assuming rate constants inversely dependent on temperature to a small power could equally well be fitted to the experimental data of Fig. 11.

Finally, it is noted that the present results for H-atom recombination rate constants are in some contrast to the results recently reported by Widawsky et al[7]. These authors also employed static pressure measurements to reveal nonequilibrium effects in nozzle expansions of dissociated H_2. In their tests they used pure H_2 initially dissociated by electric discharge, and tested at reservoir pressures around 1 atm. They do not consider different third-body effects, and their recombination-rate constants inferred tend to average substantially higher than the average of corresponding shock-wave rate constants. However, meaningful comparison with their results is difficult because of the different reservoir conditions and test-gas mixtures employed. In addition, there are certain important questions concerning the rates inferred from their experiments which are not discussed. These questions include the effect of nozzle-wall boundary layer (which though possibly having only a small effect on pressure would nevertheless have a very large effect on rate constants inferred from pressure), and the effects of the vaporized trigger wire as an impurity (possibly catalytic) influencing the flow chemistry.

5. CONCLUDING REMARKS

The present experiments were undertaken to observe thermal and chemical nonequilibrium effects in simple expansion flows characterized by a single dominant rate process. It was thereby hoped that observed effects would be reasonably definitive and could be interpreted with confidence.

The results obtained on nitrogen vibrational lag by use of the sensitive line-reversal method, i.e. that vibrational temperatures remain much closer to equilibrium during flow expansion than anticipated, were quite unexpected and have not been completely explained within the framework of existing theory. Independent confirmation of these results is clearly desirable considering the importance of vibrational relaxation as a fundamental process for the exchange of molecular energy. The present results also have a direct implication as regards the problem of vibrational relaxation in wind-tunnel nozzle flows of N_2 or air. They indicate that vibrational freezing, and consequent effects on the gas dynamics, may be much less severe than previously anticipated.

The experiments with dissociated H_2 + Ar mixtures show a definite departure from equilibrium static pressures which is interpreted as due to lag in H-atom recombination occurring in the flow expansion. The recombination rate constants inferred from the pressure data (which are dominated by that for H as the third body) lie within the range of variation of those inferred from previous shock-wave dissociation studies with similar H_2 + Ar mixtures. However, the uncertainty in the rate constants deduced, namely a factor of about 2.5, together with the spread of the shock-wave rate data could mask an appreciable difference in this respect. Further clarification requires additional studies employing diagnostic methods more sensitive to the H_2-flow chemistry than is the static pressure. Development of a spectroscopic technique for this purpose is currently underway at CAL.

APPENDIX - METHODS OF CALCULATION OF VIBRATIONAL TEMPERATURES IN EXPANSION FLOWS

The first of two methods to be described is similar to the one described in Ref. 5, and is referred to here as the macroscopic relaxation method. The second method was developed during the course of the present work, and is referred to here as the microscopic de-excitation method.

Macroscopic Relaxation Method - This method assumes the applicability of the Landau-Teller relaxation equation as used in normal shock studies. The macroscopic relaxation time τ_s from Fig. 4 is used to characterize vibrational de-excitation during pseudo-one-dimensional expansion processes. This relaxation equation is, for steady flow,

$$\frac{dE(T_v)}{dx} = \frac{E(T) - E(T_v)}{\lambda_s} \qquad (1)$$

where

$E(T_v)$ = vibrational energy at the local vibrational temperature T_v

$E(T)$ = vibrational energy which would exist at the local translational temperature T

λ_s = macroscopic characteristic relaxation length, $u\tau_s$ (τ_s evaluated at the local value of T)

x = axial distance measured from nozzle throat.

If the diatomic molecule is represented by a harmonic oscillator, the vibrational energy E is given by

$$E(T_v) = \frac{R\Theta}{(e^{\Theta/T_v} - 1)}$$

where Θ is the characteristic vibrational temperature (taken as 3374°K for N_2).

Equation (1) together with the usual gasdynamic equations and thermodynamic relations completely describe the vibrational relaxation of nitrogen in the conical nozzle without transport or wall effects. For given initial conditions and nozzle geometry, exact solutions to the system of equations can be obtained by rather laborious numerical techniques. An approximate solution to Eq. (1) above can be obtained much more readily by evaluating $E(T)$ and $\lambda_s = u\tau_s(T)$ for equilibrium flow. Generally, the effects of vibrational relaxation on the thermo-gasdynamics of the nozzle flow are sufficiently small (due to the rather small enthalpy involved) that this approximation is quite good, as demonstrated in Ref. 5. Expressing Eq. (1) in finite difference form as in Ref. 5, the vibrational energy distribution can then be determined by step-by-step computation from

$$E(T_v)_{n+1} = \frac{\left[1 - \frac{\Delta x}{2\lambda_n}\right]}{\left[1 + \frac{\Delta x}{2\lambda_{n+1}}\right]} E(T_v)_n + \frac{\Delta x/2}{\left[1 + \frac{\Delta x}{2\lambda_{n+1}}\right]}\left[\frac{E(T)_{n+1}}{\lambda_{n+1}} + \frac{E(T)_n}{\lambda_n}\right]$$

where n and $n+1$ refer to two adjacent locations along the nozzle axis separated by distance Δx, and λ and T are evaluated for equilibrium flow. It is noted that the second term on the right hand side is a function of the equilibrium flow solution only and tends to zero rather rapidly within increasing x. In the present work the results obtained by the foregoing approximate method have also been found (as in Ref. 5) to agree well with the results obtained by solving the complete system of equations by hand calculation.

Microscopic De-excitation Method - In the microscopic de-excitation method, the relaxation of the vibrational temperature is expressed in terms of the probability of vibrational de-excitation and its dependence on the local translational temperature and pressure. In this way, an expression for the local vibrational temperature is obtained in integral form, which involves the probability of de-excitation per collision as an easily adjusted independent parameter.

This method considers a multi-level vibrator with the transfer of energy between adjacent vibrational levels represented by

$$n_i + n \underset{k_{ji}}{\overset{k_{ij}}{\rightleftharpoons}} n_j + n$$

where (n_i) and (n_j) are the populations of the i th and j th levels in molecules/cm^3, and k_{ij}, k_{ji} the rates of collisional excitation and de-excitation for these respective levels. n is any N_2 molecule, so that $(n) = \sum(n_i)$. The time rate of change of (n_i) is given by

$$\rho \frac{D}{Dt}\left[\frac{(n_i)}{\rho}\right] = k_{ji}(n_j)(n) - k_{ij}(n_i)(n)$$

By considering the ratio of the population of the two lowest levels (0 and 1) it can be shown that the vibrational temperature T_v at any distance x from the nozzle throat is given by

$$\left(\frac{1}{T_v}\right)_x = \left(\frac{1}{T_v^*}\right) + \int_0^x \frac{Z\beta_{10}T^{1/2}}{\mu\Theta}\frac{\rho}{u}\frac{(1 - e^{-\Theta/T})}{(1 - e^{-\Theta/T_v})}\left[1 + \left(1 - \frac{\beta_{21}}{\beta_{10}}\right)e^{-\Theta/T_v}\right]dx \qquad (2)$$

where

T_v^* = vibrational temperature at the throat

ρ = local gas density

u = local gas velocity

T = local translational temperature

β_{21} = probability of de-excitation from level 2 to level 1 = k_{21}/Z

β_{10} = probability of de-excitation from level 1 to zero level = k_{10}/Z

Z = collision frequency, collisions per mole/cc per sec.

μ = molecular weight

In deriving Eq. (2), the assumptions made are that a Boltzmann distribution is maintained between the levels during the expansion, and that transitions occur only between adjacent levels. The first assumption is reasonably well justified, since the exchange of vibrational quanta between levels occurs about 10^6 times more efficiently than vibrational-translational exchanges. The second assumption follows that initially made by Zener[22] on the basis of the nature of the particular molecular interaction involved.

The ratio of the de-excitation probabilities β_{21}/β_{10} in the integrand of Eq. (2) is of particular interest. On the basis of the Landau-Teller theory these probabilities are proportional to the quantum number of the upper level concerned, and this ratio is thus 2. For equal probabilities the ratio is 1. In the first case, it can be shown that by expressing the vibrational temperature T_v in terms of the vibrational energy $E(T_v)$ for a simple

harmonic oscillator, the integral expression, Eq. (2), reduces to the macroscopic Landau-Teller form given by Eq. (1). This is not surprising, since the Landau-Teller probabilities are invoked in reducing the integral expression. It is interesting to note that in the second case, for equal probabilities, the integral reduces to a similar form as that for a two-level oscillator.

In an analogous manner as for Eq. (1), the integral Eq. (2) can be numerically solved to good approximation by using values for T corresponding to equilibrium flow. Values of transition probabilities for nitrogen have been collected and plotted for a range of translational temperature by Rudin[23]. The results of calculations by this approximate method using the transition probabilities of Ref. 23 and assuming $P_{21}/P_{10}=2$ are in agreement with the results calculated from the macroscopic method, Eq. (1). It may be noted that for equal probabilities, or $P_{21}/P_{10}=1$, the calculated vibrational temperatures are only slightly lower, namely about 3%, than those for $P_{21}/P_{10}=2$ for a typical case.

REFERENCES

1. Russo, A., Hurle, I., Lordi, J. and Hall, J. G., 1962, Bull. Amer. Phys. Soc., 7, 447.
2. Bray, K. N. C., 1959, J. Fluid Mech., 6, 1.
3. Hall, J. G. and Russo, A. L., 1960, Proc. First Conf. on Kinetics, Equilibria, and Performance of High Temperature Systems, Butterworths Sci. Pub., 219
4. Eschenroeder, A. Q., Boyer, D. W., and Hall, J. G., 1962, Phys. of Fluids, 5, 615.
5. Stollery, J. L. and Smith, J. E., 1962, J. Fluid Mech., 13, 225.
6. Nagamatsu, H. T., Workman, J. B. and Sheer, R. E., Jr., 1961, Jour. Aero. Sp. Sci., 28, 833.
7. Widawsky, A., Oswalt, L. R., and Harp, J. L., Jr., 1962, ARS Jour., 32, 1927.
8. Hoglund, R., Carlson, D., and Byron, S., 1963, AIAA Jour., 1, 324.
9. Blackman, V. H., 1956, J. Fluid Mech., 1, 61.
10. Gaydon, A. G., and Hurle, I. R., 1963, The Shock Tube in High-Temperature Chemical Physics, Reinhold, New York, 162.
11. de Vos, J. C., 1954, Physica, 20, 690.
12. Mitchell, A.C.G., and Zemansky, M.W., 1961, Resonance Radiation and Excited Atoms, Cambridge University Press, 187.
13. Gaydon, A. G., and Hurle, I. R., 1961, Proc. Roy. Soc. A., 262, 38.
14. Gaydon, A. G., 1960, Flames -- Their Structure, Radiation and Temperature, Chapman and Hall, London, 224.
15. Laidler, K. J., 1955, The Chemical Kinetics of Excited States, Clarendon Press, Oxford.
16. Karl, G. and Polanyi, J. C., 1963, J. Chem. Phys., 38, 271.
17. Gaydon, A. G., and Hurle, I. R., 1962, Eighth Symposium on Combustion, Williams and Wilkins Co., Baltimore, 309.
18. Hooker, W. J. and Millikan, R. C., 1963, J. Chem. Phys., 38, 214.
19. Bashenova, T. V., 1963, Soviet Physics - Doklady, 7, 783.
20. Landau, L. and Teller, E., 1936, Phys. Z. Soviet Union, 10, 34.
21. Clouston, J. G., Gaydon, A. G. and Hurle, I. R., 1959, Proc. Roy. Soc. A., 252, 143.
22. Zener, C., 1931, Phys. Rev. 37, 556.
23. Rudin, M., 1958, Phys. Fluids, 1, 384.
24. Cottrell, T. L. and McCoubrey, J. C., 1961, Molecular Energy Transfer in Gases, Butterworths, London, 135 and 129.
25. Hall, J. G., Eschenroeder, A. Q. and Klein, J. J., 1960, ARS Jour., 30, 188.
26. Sutton, E., 1962, J. Chem. Phys., 36, 2923.
27. Patch, R. W., 1962, J. Chem. Phys., 36, 1919.
28. Rink, J. P., 1962, J. Chem. Phys., 36, 262.
29. Eschenroeder, A. Q. and Lordi, J. A., 1963, Ninth Symposium on Combustion, Academic Press, New York, 241.
30. Burke, A. F., CAL Rept. No. 118, November 1961.
31. Huber, P. W. and Kantrowitz, A., 1947, J. Chem. Phys., 15, 275.
32. Lukasik, S. J. and Young, J. E., 1957, J. Chem. Phys., 27, 1149.
33. Bauer, S. H. and Tsang, S. C., 1963, Phys. Fluids, 6, 182.

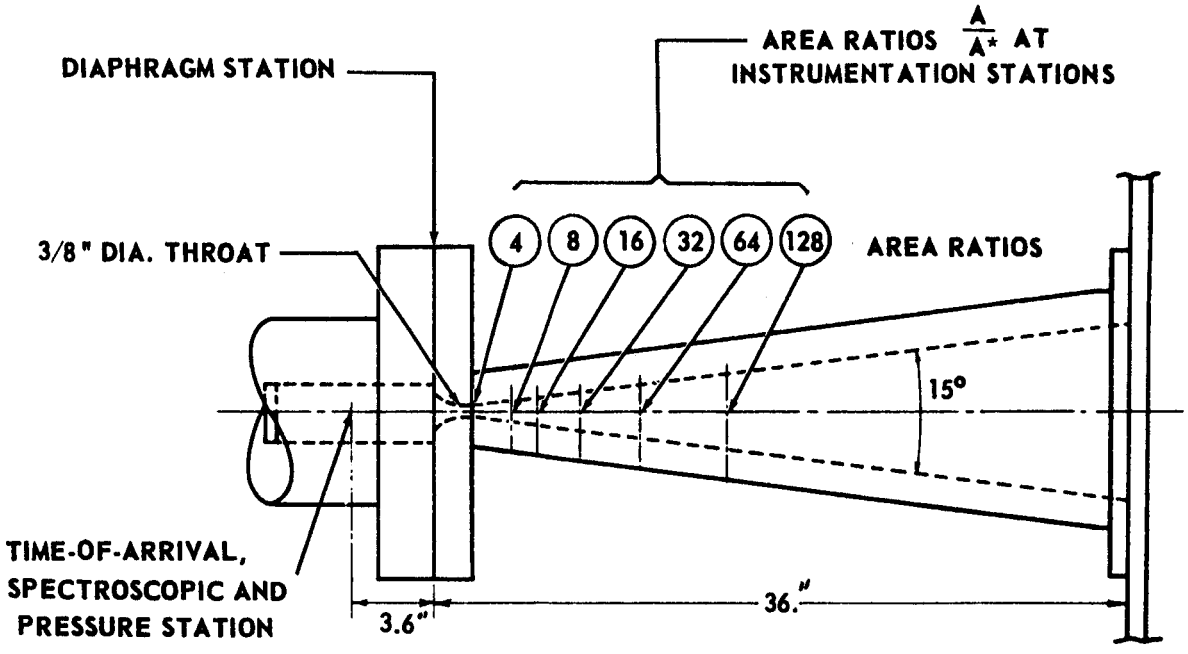

15° CONICAL NOZZLE

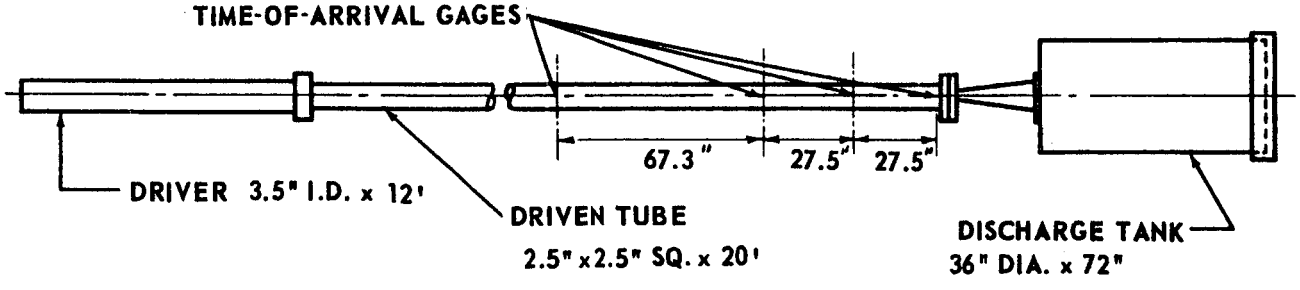

Figure 1 SHOCK TUBE-NOZZLE-DISCHARGE TANK ASSEMBLY

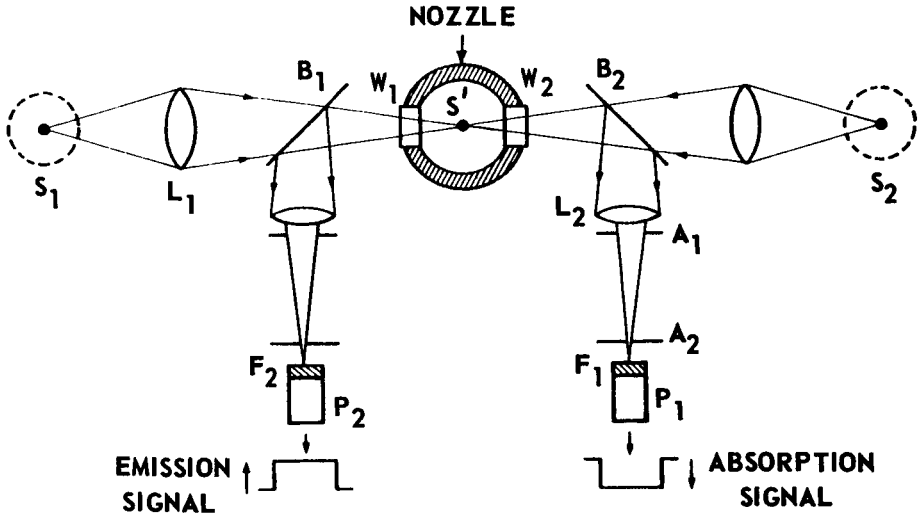

(a) AXIAL VIEW OF OPTICAL ARRANGEMENT OF ONE DOUBLE-BEAM SYSTEM

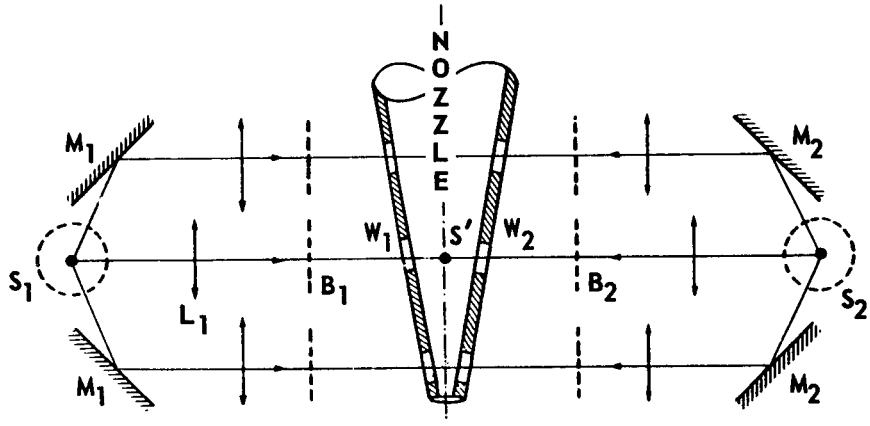

(b) PLAN VIEW OF ARRANGEMENT OF BEAMS FOR THREE STATIONS IN THE NOZZLE

Figure 2 OPTICAL SYSTEM FOR SPECTRUM-LINE REVERSAL MEASUREMENTS

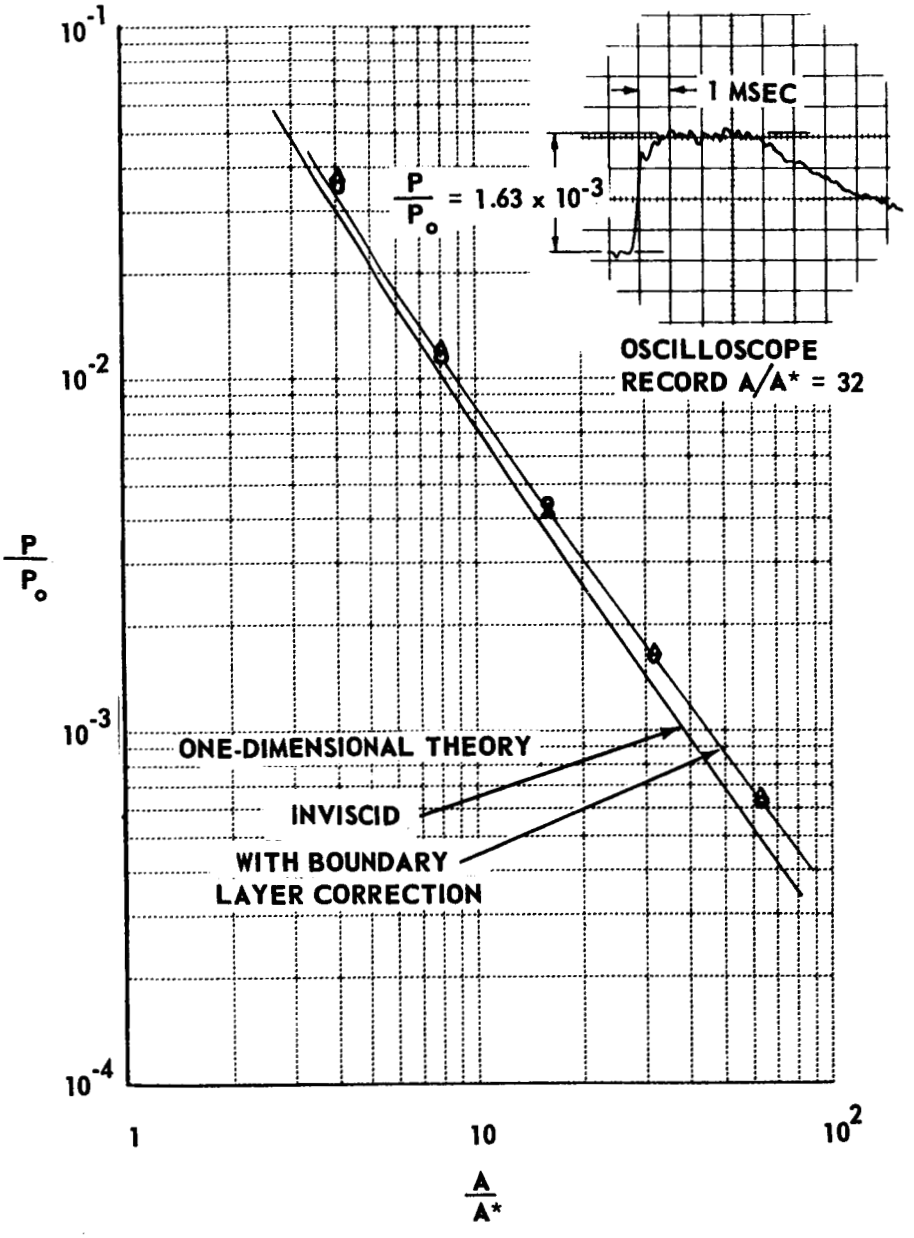

Figure 3 TYPICAL PRESSURE DATA MEASURED IN CALIBRATION EXPERIMENTS TO ASSESS BOUNDARY LAYER EFFECTS IN 15° CONICAL NOZZLE
N_2, T_o = 2000°K, P_o = 60 ATM

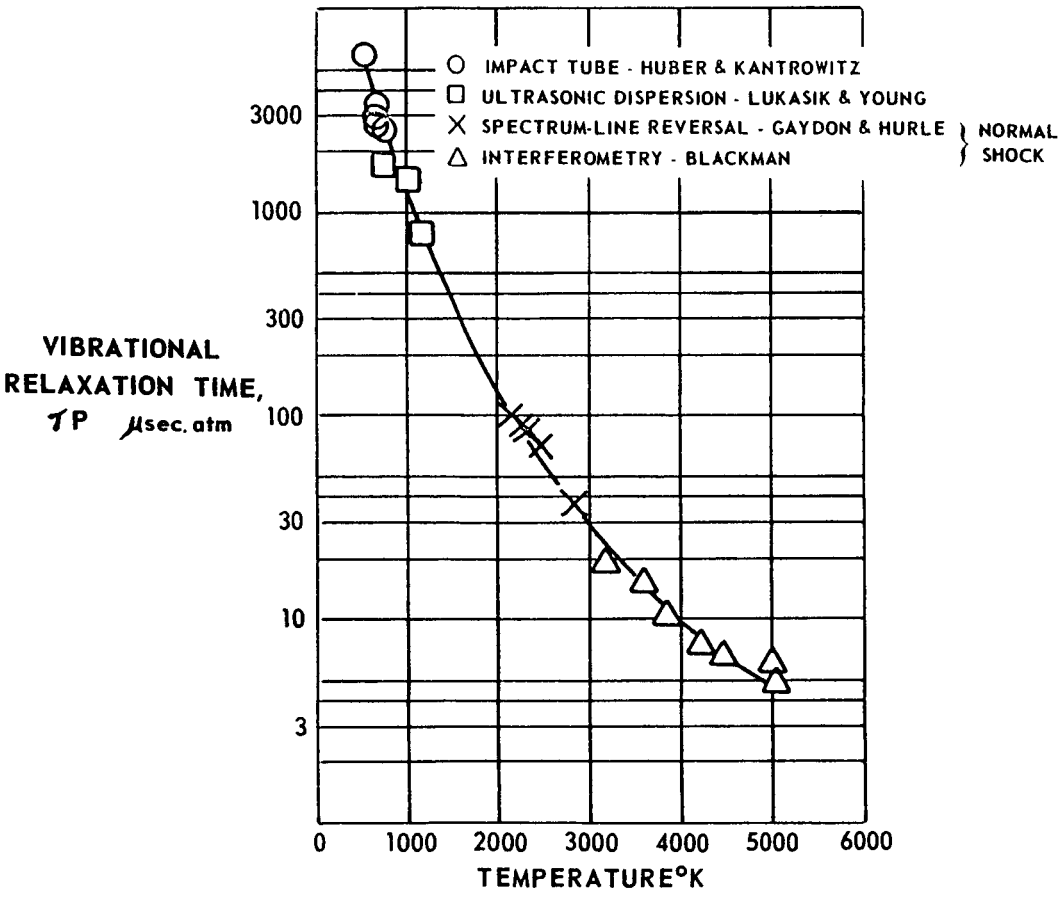

Figure 4 PREVIOUS VIBRATIONAL RELAXATION DATA FOR N_2 INCLUDING NORMAL -SHOCK RESULTS

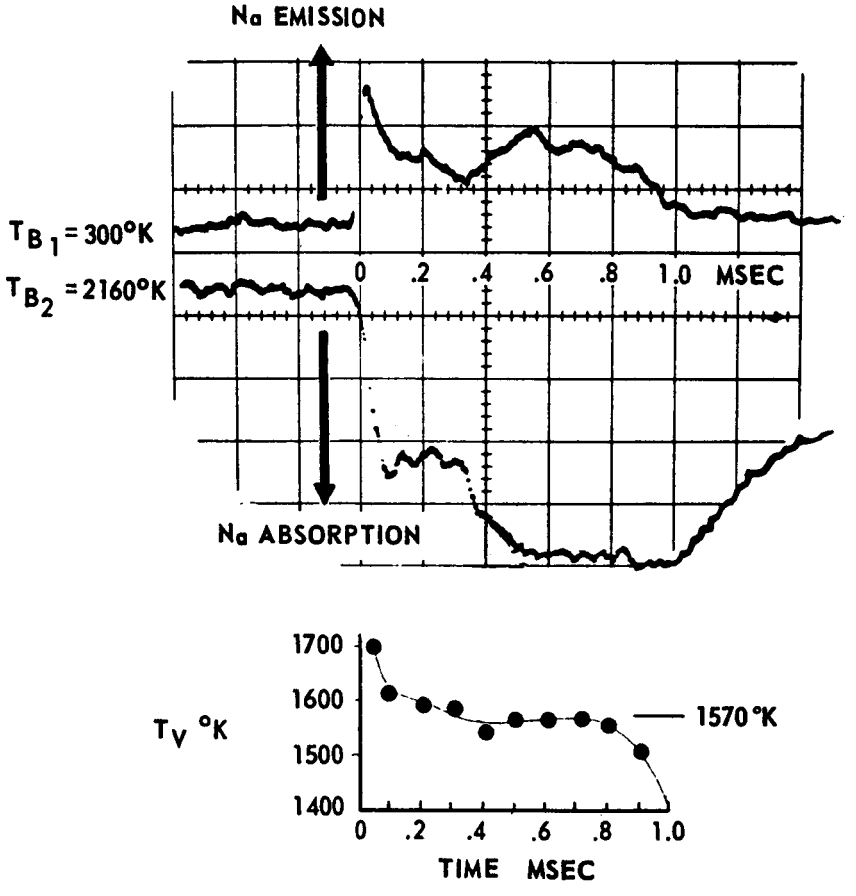

Figure 5 TYPICAL DOUBLE-BEAM RECORD OF REVERSAL TEMPERATURE MEASUREMENT IN NOZZLE FOR N_2
T_o = 2800°K, P_o = 53 ATM, A/A* = 8

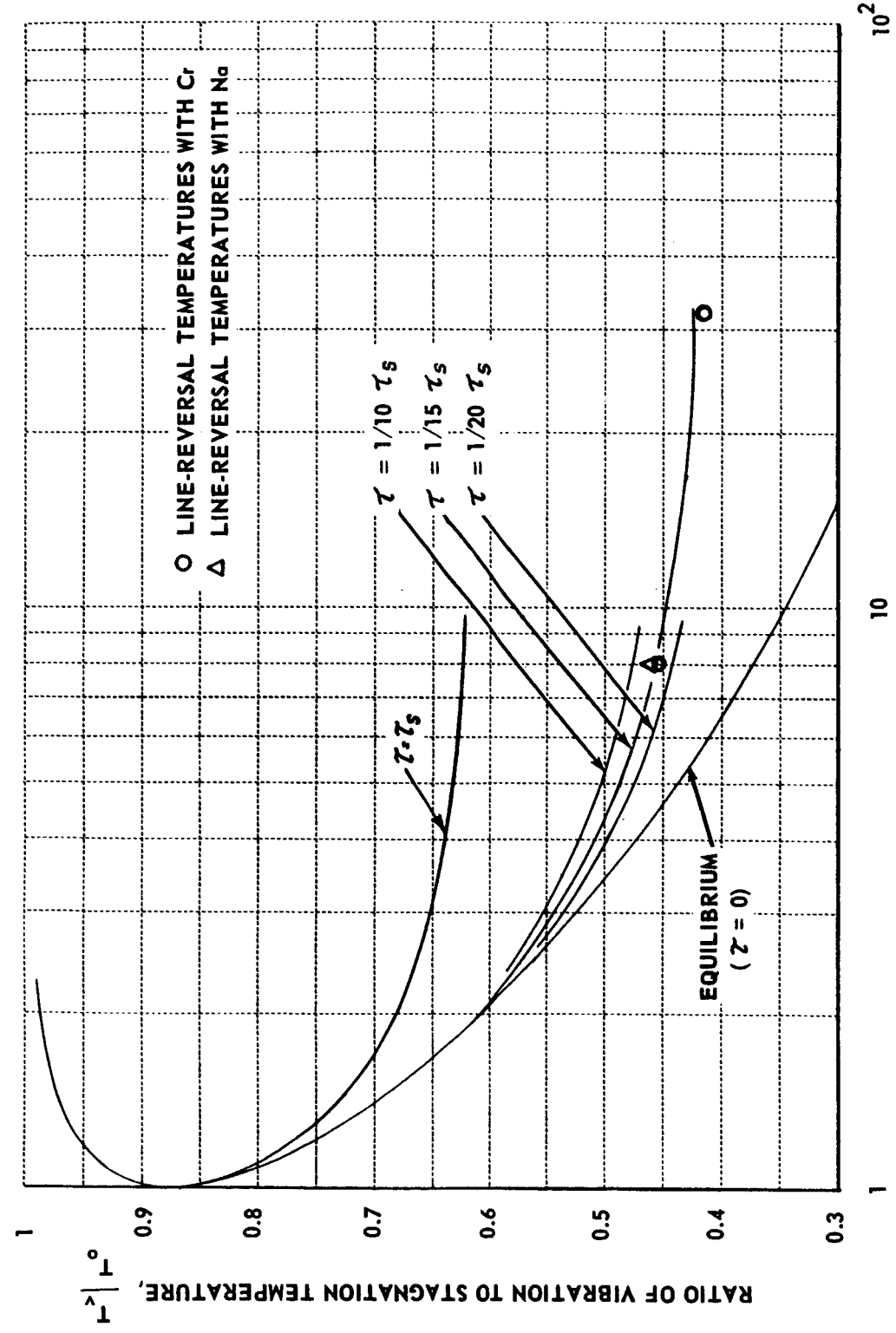

FIGURE 6 COMPARISON OF TYPICAL MEASURED VIBRATIONAL TEMPERATURES WITH THEORY FOR N_2 EXPANSIONS IN 15° CONICAL NOZZLE.

T_o = 4500 °K, P_o = 50 ATM

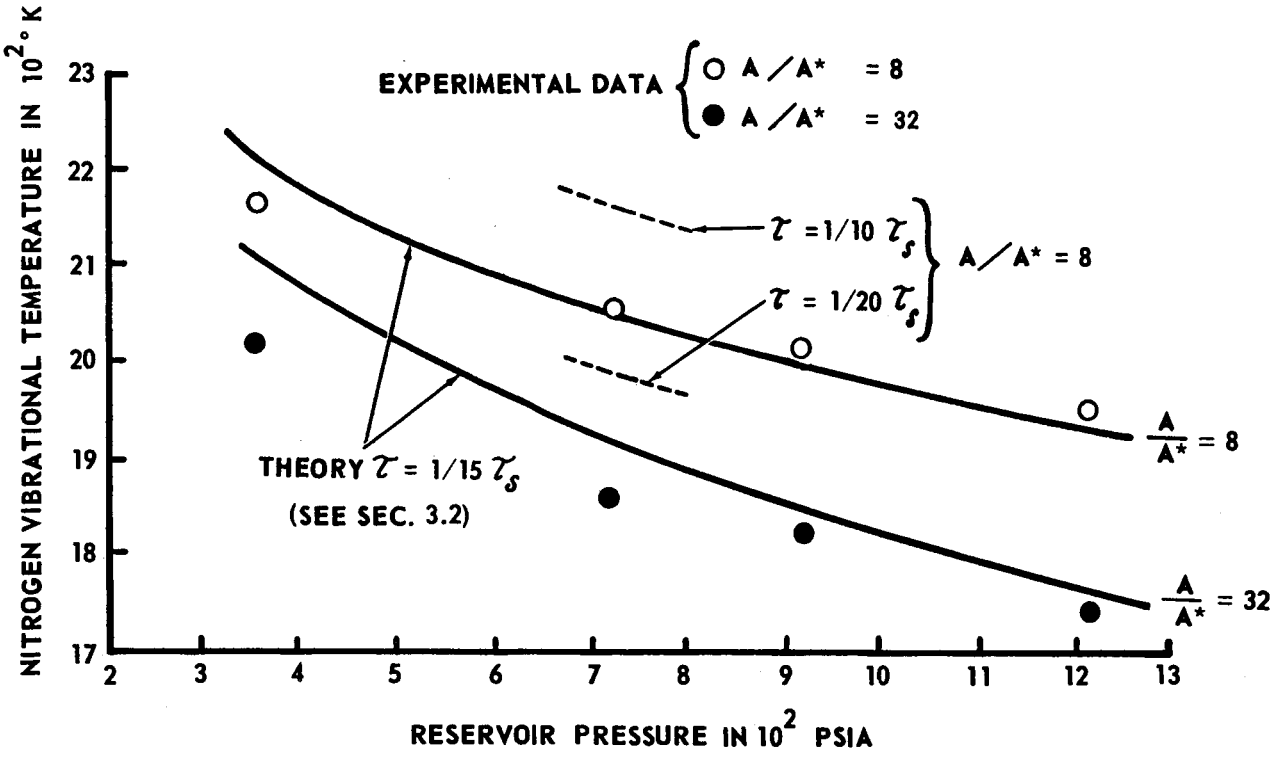

Figure 7 EFFECT OF RESERVOIR PRESSURE ON EXPERIMENTAL AND THEORETICAL VIBRATIONAL TEMPERATURES OF N_2 EXPANSIONS IN 15° CONICAL NOZZLE. T_o = 4500°K

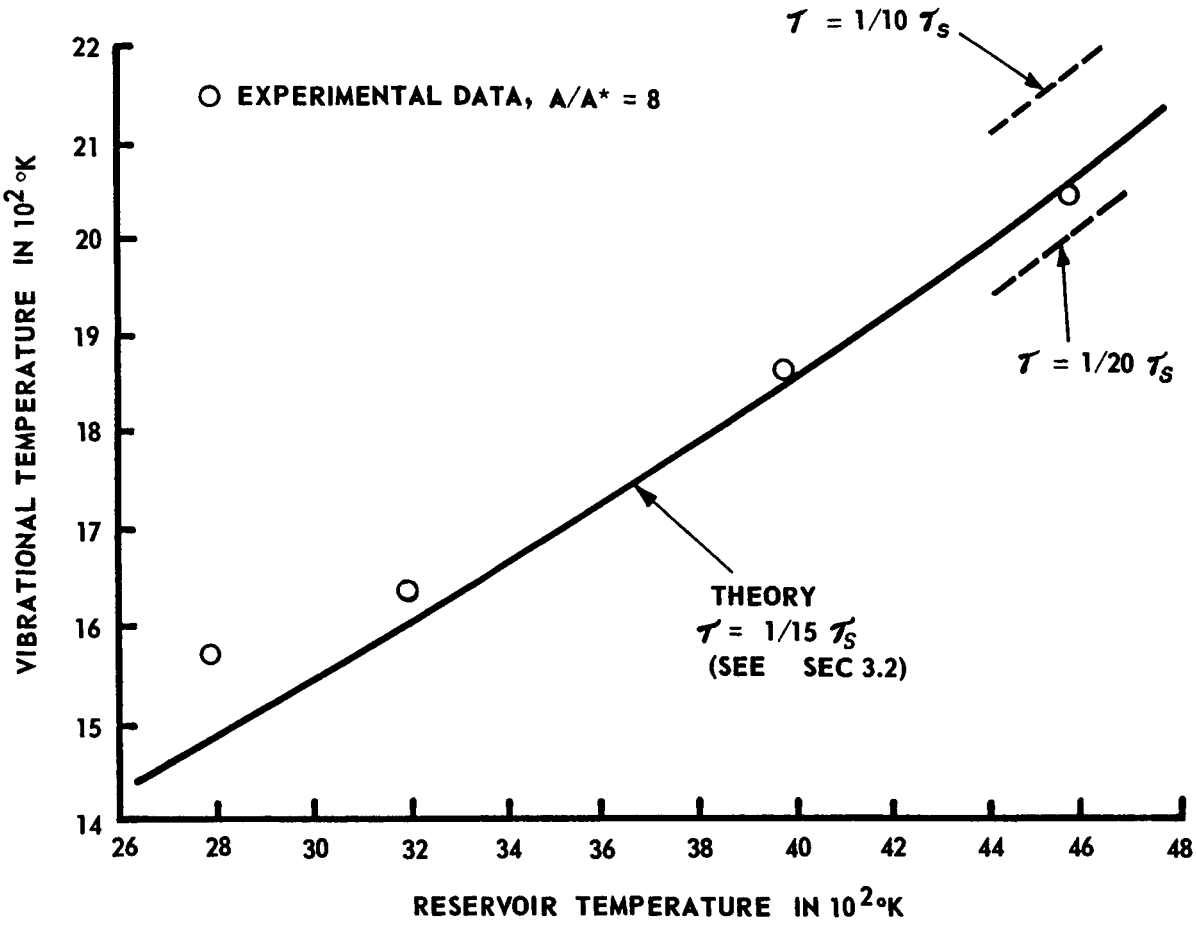

Figure 8 EFFECT OF RESERVOIR TEMPERATURE ON EXPERIMENTAL AND THEORETICAL VIBRATIONAL TEMPERATURES FOR N_2 EXPANSIONS IN 15° CONICAL NOZZLE. P_o = 50 ATM

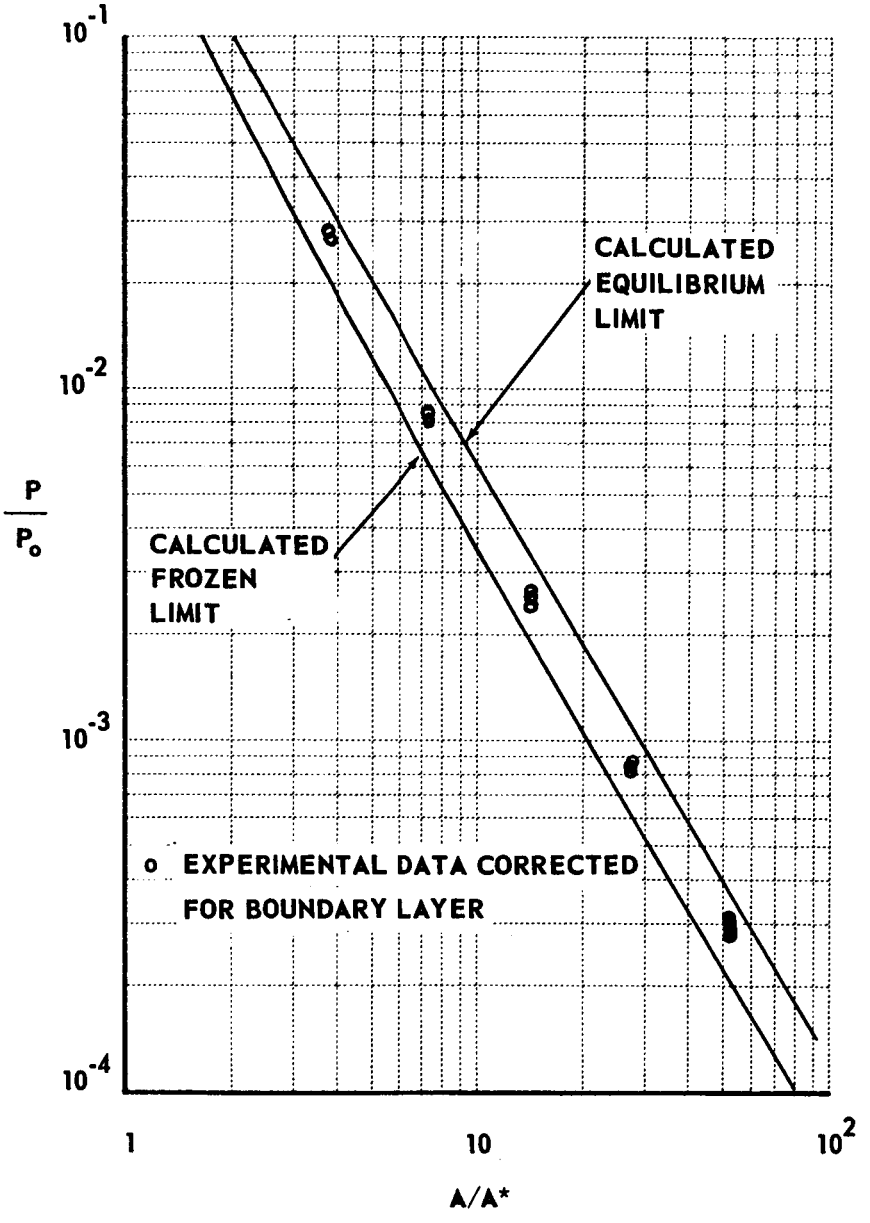

FIGURE 9 MEASURED PRESSURE DISTRIBUTION FOR FLOW OF DISSOCIATED H_2-Ar MIXTURE IN 15° CONICAL NOZZLE. T_o = 6000 °K, P_o = 57 ATM UNDISSOCIATED MIXTURE 7.95% H_2 + 92.05% Ar

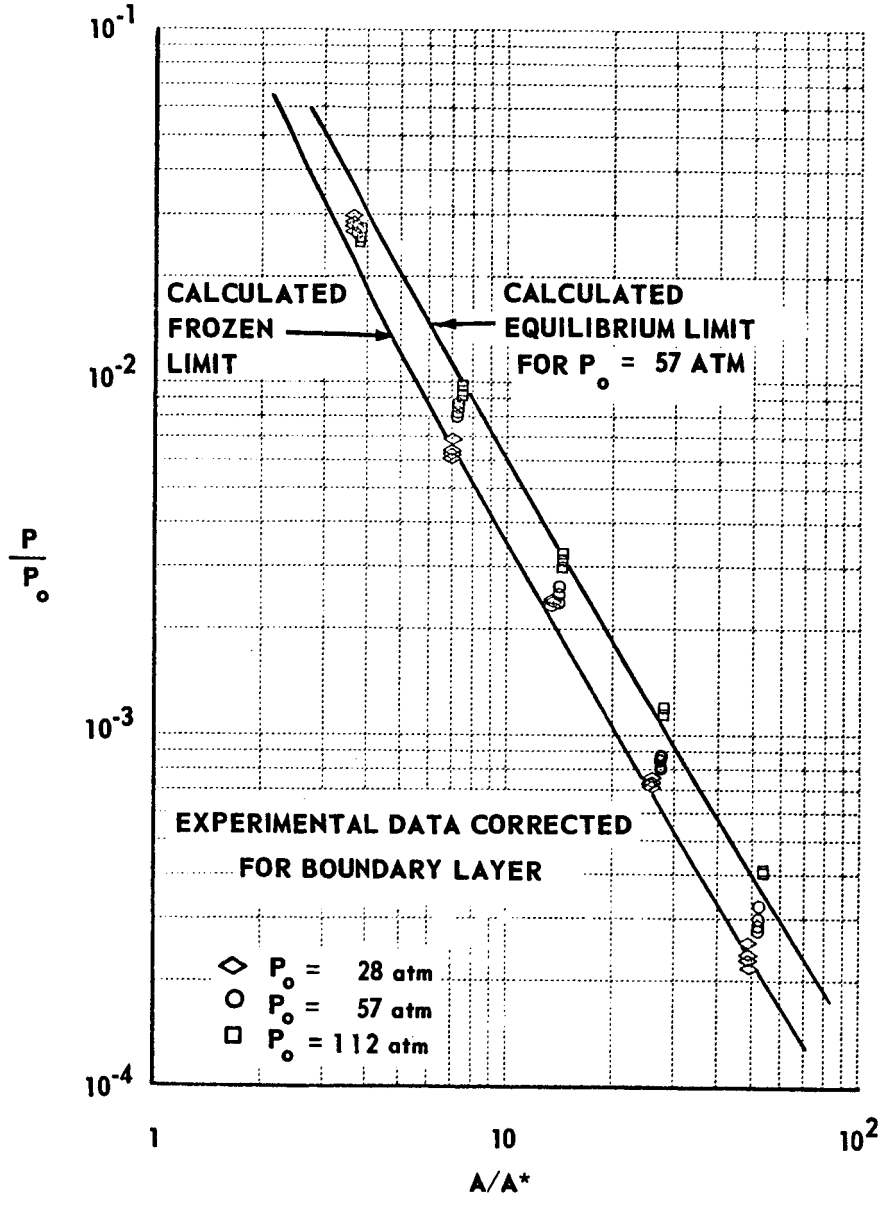

FIGURE 10 EFFECT OF RESERVOIR PRESSURE P_o ON MEASURED PRESSURE DISTRIBUTIONS FOR FLOW OF DISSOCIATED H_2-Ar MIXTURE IN 15° CONICAL NOZZLE. T_o = 6000°K. UNDISSOCIATED MIXTURE 7.95% H_2 + 92.05% Ar.

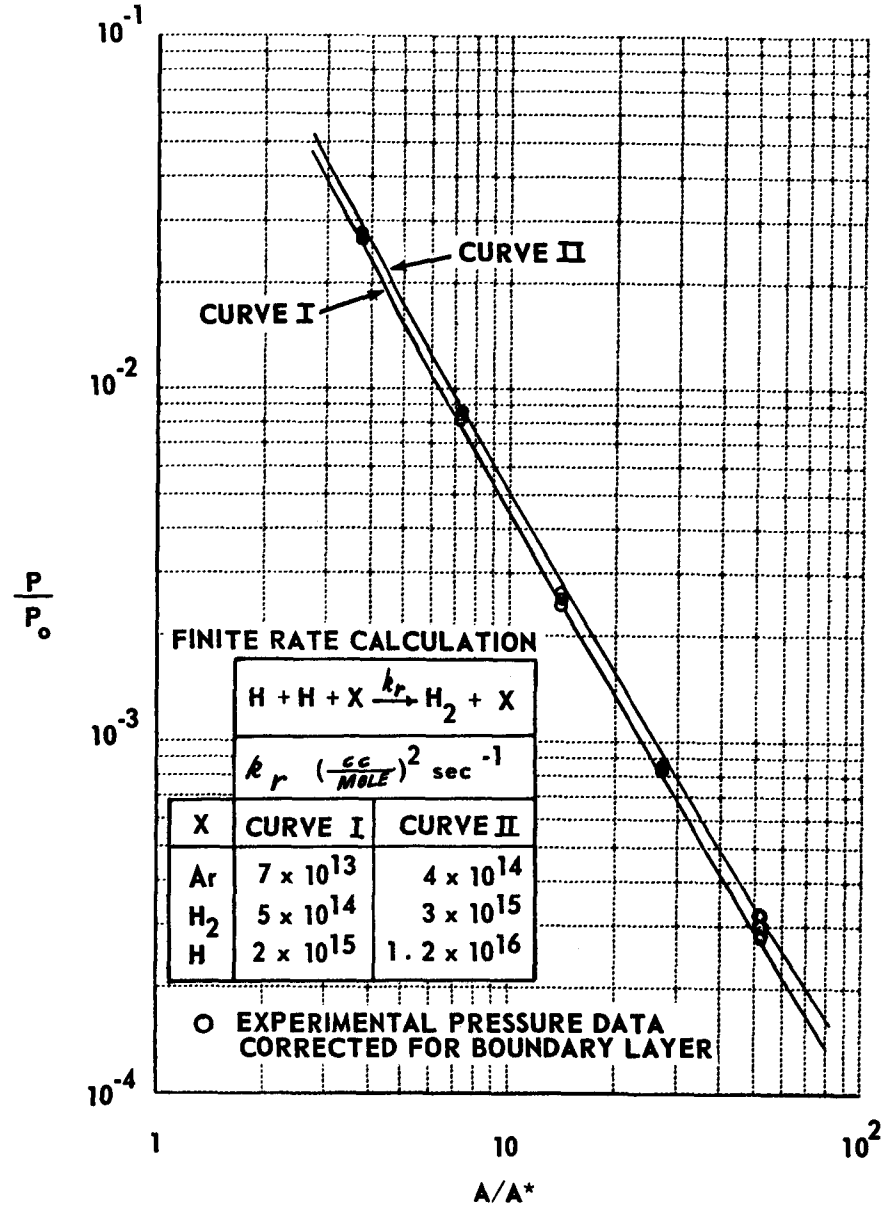

FIGURE 11 COMPARISON OF MEASURED PRESSURE DISTRIBUTIONS WITH FINITE RATE CALCULATIONS FOR FLOW OF DISSOCIATED H_2 + Ar MIXTURE IN 15° CONICAL NOZZLE. T_o = 6000°K, P_o = 57 ATM UNDISSOCIATED MIXTURE 7.95% H_2 + 92.05% Ar

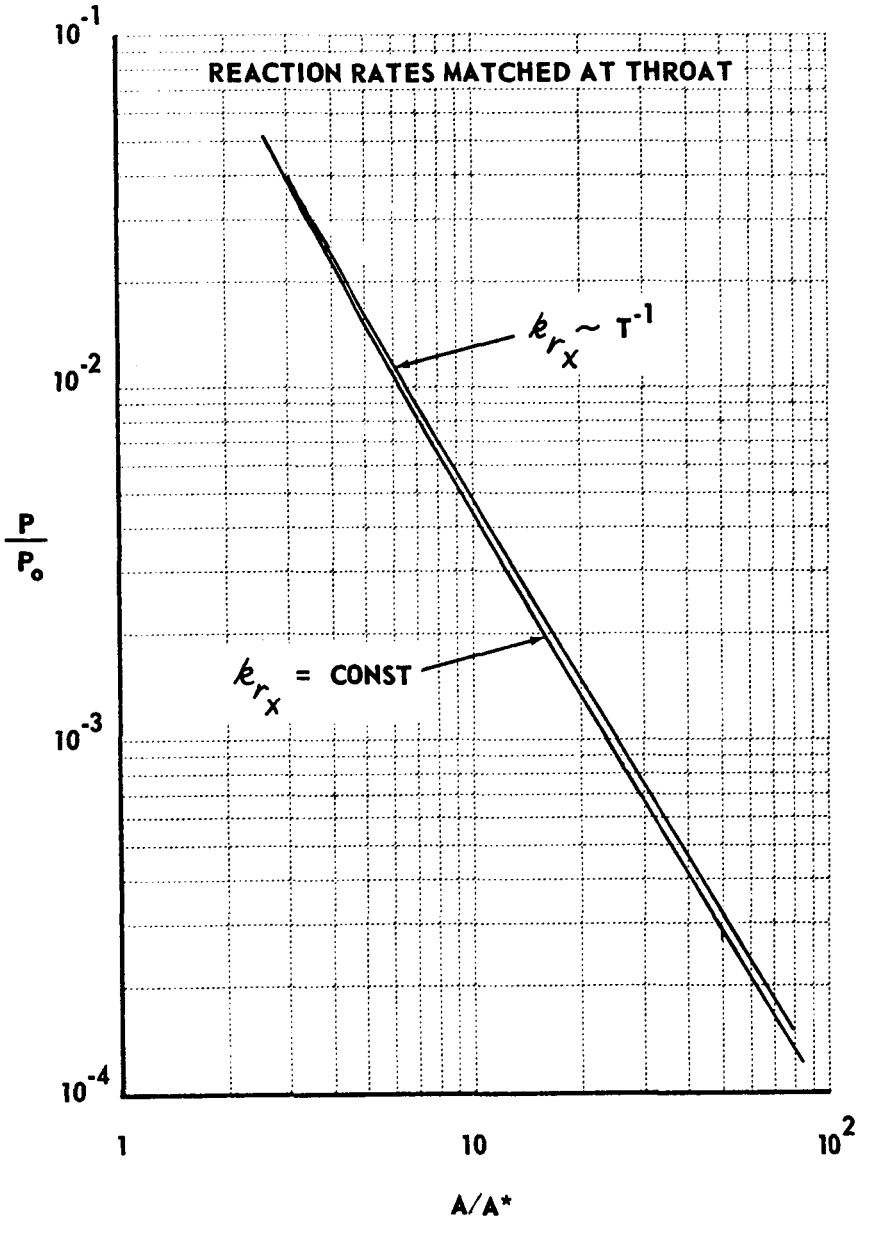

FIGURE 12 EFFECT OF TEMPERATURE DEPENDENCY OF REACTION RATES ON CALCULATED FINITE RATE FLOW OF DISSOCIATED H_2-Ar MIXTURE IN CONICAL NOZZLE. T_o = 6000°K P_o = 57 ATM UNDISSOCIATED MIXTURE 7.95% H_2 + 92.05% Ar